EPSC2018

LFI3 abstracts

EPSC Abstracts
Vol. 12, EPSC2018-24, 2018
European Planetary Science Congress 2018

Irradiation of meteorites: decoding space weathering on low albedo asteroids

Cateline Lantz and **Rosario Brunetto**
Institut d'Astrophysique Spatiale, CNRS/Univ. Paris Saclay, Bât. 121, Campus Paris Sud, 91405 Orsay, France
(rosario.brunetto@ias.u-psud.fr)

Abstract

Space weathering (SpWe) processes such as micrometeorite bombardment or solar wind ion irradiation produce changes on the surface of airless bodies, impeding us to decipher their composition from their spectra. This effect has been widely studied for the case of the Moon and S-type asteroids and is now investigated for primitive asteroids [1].

In order to understand the influence of SpWe on carbonaceous materials and to support current sample return missions (Hayabusa2/JAXA and OSIRIS-REx/NASA), we performed 40 keV He^+ and Ar^+ ion irradiation of carbonaceous chondrites (CCs) as a simulation of solar wind irradiation of C-complex asteroids. We used reflectance spectroscopy (0.4-16 µm) to probe our samples.

We studied several types of CCs [2-4] as they span a wide range of albedos (from 2-5% for CI/CM to 15-18% for CV/CO), initial composition (matrix- or chondrules-rich) and did not suffer the same thermal history (aqueous alteration or metamorphism). We proposed new insights on the effects of SpWe on low albedo asteroids based on these experiments. We recently performed new irradiation experiments on other meteorites (CK, CR and CM with different degrees of aqueous alteration) to test further our model. We will present the new results and discuss them regarding our previous study.

Micro-reflectance spectra were also acquired (2.5-12 µm) using a spot size of 20 µm and scanning large areas (from mm^2 to cm^2) of the samples (13 mm diameter pellets), both on virgin and irradiated areas (see Fig.1). Spectral maps allowed us characterizing the heterogeneity of the meteorites at the 20 µm spatial scale [5].

Compositional heterogeneity of the pristine materials and irradiation effects were compared to each other as a function of the irradiation dose, to determine which spectral features are more sensitive to SpWe. Results were then compared with the IR spectral capabilities of instruments onboard Hayabusa2 and OSIRIS-REx, to provide these missions with spectral criteria on how to distinguish SpWe from compositional heterogeneity effects at the asteroid, and in view of surface selection for sample return.

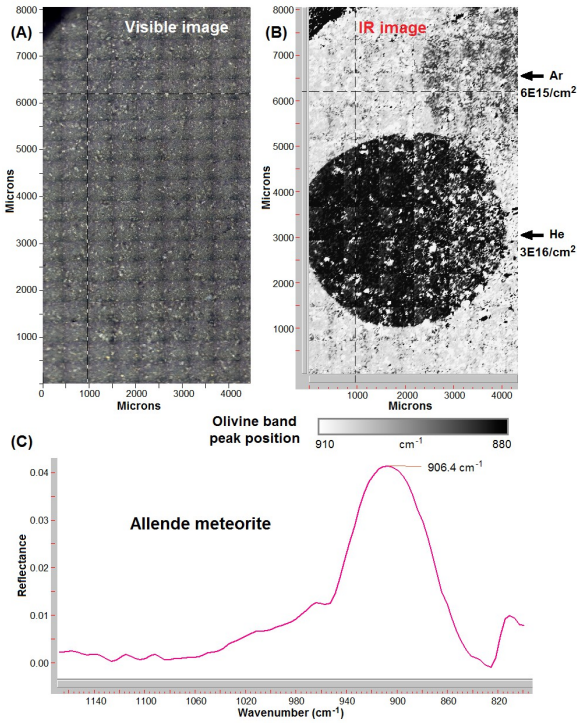

Figure 1: Mid-IR spectral imaging of the Allende meteorite, with two irradiation spots at different ion dose. Panel (A): visible image showing the typical heterogeneous composition of the meteorite pellet. Panel (B): IR map showing the peak position of the 11-µm band in gray scales, with white for short and black for long wavelength peak position. Panel (C): a typical matrix spectrum of Allende with the prominent 11-µm anhydrous silicates band collected on one spot of ~20 µm.

Acknowledgements

We are grateful to the teams at IAS, SOLEIL, CSNSM, LESIA and IPAG for valuable support, help and discussion. We thank P. Beck, É. Quirico, and the Vatican Observatory for the samples. The micro-spectroscopy activities were supported by grants from Région Ile-de-France (DIM-ACAV) and SOLEIL. The irradiations were performed using the INGMAR setup, a joint IAS-CSNSM (Orsay, France) facility funded by the Programme National de Planétologie (PNP), by the Faculté des Sciences d'Orsay, Université Paris-Sud (Attractivité 2012), by the French National Research Agency ANR (contract ANR-11-BS56-0026, OGRESSE), and by the P2IO LabEx (ANR-10-LABX-0038) in the framework Investissements d'Avenir (ANR-11-IDEX-0003-01). This work was supported by the CNES. It is related to observations performed with NIRS3 embarked on Hayabusa2 (JAXA).

References

[1] Brunetto, R., Loeffler, M.J., Nesvorny, D., Sasaki, S., Strazzulla, G.: Asteroid Surface Alteration by Space Weathering Processes, in Asteroids IV, pp. 597-616, 2015.

[2] Brunetto, R., and 15 colleagues: Ion irradiation of Allende meteorite probed by visible, IR, and Raman spectroscopies, Icarus, Vol. 237, pp. 278-292, 2014.

[3] Lantz, C., Brunetto, R., Barucci, M.A., Dartois, E., Duprat, J., Engrand, C., Godard, M., Ledu, D., Quirico, E.: Ion irradiation of the Murchison meteorite: Visible to mid-infrared spectroscopic results, Astronomy and Astrophysics Vol. 577, A41, 2015.

[4] Lantz, C., Brunetto, R., Barucci, M.A., Fornasier, S., Baklouti, D., Bourçois, J., Godard, M.: Ion irradiation of carbonaceous chondrites: A new view of space weathering on primitive asteroids, Icarus, Vol. 285, pp. 43-57, 2017.

[5] Brunetto, R., Lantz, C., Dionnet, Z., Borondics, F., Aléon-Toppani, A., Baklouti, D., Barucci, M.A., Binzel, R.P., Djouadi, Z., Kitazato, K., Pilorget, C.: Hyperspectral FTIR imaging of irradiated carbonaceous meteorites, Planetary and Space Science, 2018 submitted.

EPSC Abstracts
Vol. 12, EPSC2018-34, 2018
European Planetary Science Congress 2018

Nature and occurrence frequency of heating processes in CM and C2-ungrouped chondrites as revealed by insoluble organic matter

E. Quirico[1], L. Bonal[1], P. Beck[1], C.M.O'D. Alexander[2], H. Yabuta[3], T. Nakamura[4], A. Nakato[5], L. Flandinet[1], G. Montagnac[6], P. Schmitt-Kopplin[7] and C. Herd[8], [1]IPAG UGA France, [2]DTM Carnegie Institution Washington USA, [3]Hirosima University Japan, [4]Tohoku University, Sendai, Miyagi 980-8578, Japan, [5]Institute of Space and Astronautical Science, Japan Aerospace Exploration Agency, Sagamihara,Japan, [6]Laboratoire de Géologie de Lyon, CNRS, Ecole Normale Supérieure de Lyon, 46 allée d'Italie – BP 7000, 69342 Lyon Cedex 07, France [7]Helmholtz-Zentrum Muenchen-German Research Center for Environmental Health, Institute for Ecological Chemistry, Ingolstaedter Landstrasse 1, D-85764 Oberschleißheim, Germany. [8]Department of Earth and Atmospheric Sciences, University of Alberta, Edmonton, Alberta T6G 2E3, Canada

Abstract

Here we report a Raman and infrared study of the composition and structure of Insoluble Organic Matter (IOM) in a series of 39 CM and C2-ungrouped chondrites. These parameters are tracers of the extent and nature of thermal metamorphism a meteorite has experienced. We propose a carbon-based classification of heated C2 chondrites that reveals a high occurrence frequency of thermally processed C2 chondrites (> 36 %). The post-accretional history is discussed thoroughly for a number of chondrites, and we propose that impacts constitute the major heating (against solar heating).

1. Introduction

Chondrites are exhumed from the interiors of their parent bodies by impacts, which at the same time can result in heating and mechanical modification (compaction, deformation, fracturing, etc.). However, whether impacts are responsible for the occurrence of heated C2s remains controversial since radiogenic and solar heating have also been invoked to explain them [1,2]. Here we report a Raman and infrared study of the composition and structure of Insoluble Organic Matter (IOM) in a series of 39 CM and C2-ungrouped chondrites. These parameters are tracers of the extent and nature of thermal metamorphism a meteorite has experienced and reflect the degree to which the thermally driven and irreversible carbonization of IOM has proceeded.

2. Results and discussion

IR measurements distinguish two groups of chondrites: R1 as primitive unheated and R2 as heated. Heating effects result mostly as an increase of the CH_2/CH_3 ratio, a loss of carbonyl groups and overall and aromatization. Raman data reveal three groups: R1, composed mainly of primitive objects; R2, slightly heated chondrites and R3, mildly heated chondrites (Fig. 1).

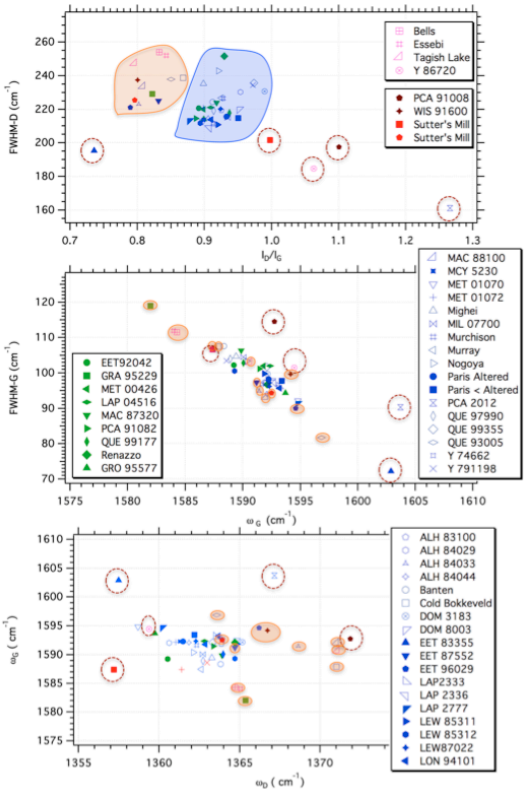

Figure 1: Raman spectral parameters revealing the groups R1 (blue are), R2 (orange) and R3 (detached in top.

Based on combinations of IR and R groups, we propose a carbon-based classification of heated C2

chondrites that reveals a high occurrence frequency of thermally processed C2 chondrites (> 36 %) (Tab.1). This classification is in agreement with the mineralogical classification scheme of [3]. Strongly heated C2 chondrites (PCA 02012, PCA 91008, Y 96720) display an IOM structural evolution that is dissimilar to that of type 3 chondrites that experienced long duration radiogenic thermal metamorphism. These differences almost certainly reflect kinetic constraints on IOM modification during short duration heating events. QUE 93005 is a weakly heated chondrite that experienced a retrograde aqueous alteration. Its very aliphatic-rich IOM points to a parent body hydrogenation through interactions with water. The closed-system conditions required by this mechanism could be satisfied by a *kinetic confinement* during a very short duration impact. MET 01072, a heavily compacted and uni-axially deformed chondrite, did not experience post-accretional heating. In this case, the deformation features probably reflect a low-velocity impact. In contrast, the weakly metamorphosed chondrite EET 96029 experienced one or several low pressure impacts that triggered mild heating and partial dehydration without deformation features.

The study of a series of lithologies from the Tagish Lake C2-ungrouped chondrite confirms the coexistence of various degrees of post-accretional alteration, the most altered lithologies having experienced a moderate degree of heating. Overall, the high prevalence of heating in C2 chondrites, the evidence of short-duration heating in the most heated C2s and the ability of low velocity collisions to trigger heating favor impacts (against solar heating) as the dominant heating mechanism. Finally, our set of data does not support the action of a low temperature oxidation process that would control the aliphatic abundance in unheated primitive C2s.

Table 1: C2 chondrites taxonomy based on IOM structure and composition.

R1:IR1 TI[1]	R2:IR2 TIII/IV[1]	R3:IR2 TII[1]	R1:IR2 TII[1]	R3:IR1 ?	Unclassified
ALH 84044	EET 83355	ALH 84033	MIL 07700	Bells	ALH 84029
ALH 83100	PCA 2012	Cold Bokkeveld		Essebi	Mighei
DOM 3183	PCA 91008	EET 87522			Murray
DOM 8003	Y 86720	EET 96029			LAP 2333
LAP 2777		MAC 88100			LAP 2336
LEW 85311		QUE 9300596.			Y 74662
LEW 85312		WIS 91600			Y 791198
LEW 87022		Tagish Lake 11h, 11i, 4, 10a			
LON 94101		Y793321			
MCY 05230					
MET 01070					
MET 01072					
Murchison					
Nogoya					
Paris altered					
Paris less altered					
QUE 97990					
Tagish Lake 5b					

[1]Classification of Nakamura (2005).

References

[1] Lindgren, P. et al. (2015). *Geochim. Cosmochim. Acta* 148, 159–178.

[2] Nakato, A., et al. (2008). *Earth Planets Space 60*, 855–864.

[3] Nakamura, T. (2005). *J. Mineral. Petrol. Sci.* 100, 260–272.

EPSC Abstracts
Vol. 12, EPSC2018-99, 2018
European Planetary Science Congress 2018

The Stirling Planetary Ices Laboratory within the Stirling Centre for Astromaterials Research

Axel Hagermann, Erika Kaufmann, Nicholas O. Attree, Christian Schröder and Alastair Tait
Department of Biological and Environmental Sciences, University of Stirling (axel.hagermann@stir.ac.uk)

Summary

We present the Stirling Planetary Ices Laboratory, an environmental simulation facility that has been, and can be used for a wide range of planetary science applications. The laboratory is a facility of the Stirling Centre for Astromaterials Research (SCAR).

1. Introduction

The Stirling Planetary Ices Laboratory is used to investigate thermophysical processes of planets and minor bodies. Its facilities have been used to simulate the environmental conditions on Earth, Mars, comets and asteroids.

2. Equipment

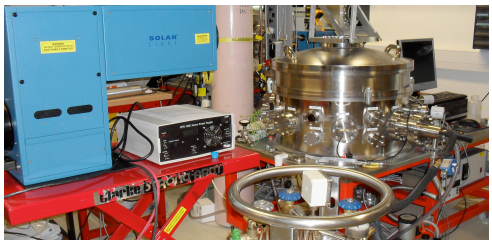

Figure 1: Standard setup for comet simulations with solar simulator to the left and DTVC to the right.

The equipment available for investigations (Figure 1) includes:

1. Dirty thermal vacuum chamber (DTVC) with cold shroud, capable of maintaining atmospheric pressures from 10^{-5} to 10^{3} mbar at temperatures as low as -140ºC. Mars atmospheric conditions can be maintained for periods exceeding several days;
2. LS1000R3 1000W Full Spectrum Solar Simulator to provide controlled solar input with zero airmass;
3. Ice making equipment for producing water and carbon dioxide ices of various morphologies;
4. Cold storage equipment for temperatures from -86ºC to room temperature;
5. Thermal and mechanical measurement suite.

3. Case studies

The Planetary Ices Laboratory was used to investigate light transmission through Mars dust contaminated snow under terrestrial atmospheric conditions [1]. It has also enabled us to verify theoretical models of arachneiform morphology on Mars [2]. Another application was the establishment of an important boundary condition for Mars atmospheric models, namely the e-folding scale of CO_2 ice [3]. The laboratory was also able to provide supporting measurements for the Rosetta mission, demonstrating subsurface ice hardening and dust agglomeration [4].

4. Future work

Currently, the Planetary Ices Laboratory is being used to run thermal simulations in support of the Hayabusa2 mission [5]. We plan to further explore the thermal processes on Mars, particularly in relation to the martian polar caps. The facility is available for collaborative projects. Please contact any of the authors to express an interest.

Acknowledgements

Funding for the Planetary Ices Laboratory is provided by STFC and the UK Space Agency under grant numbers ST/S001271 and ST/R001375.

References

[1] E. Kaufmann & A. Hagermann, 2015: Penetration of solar radiation into pure and Mars-dust contaminated snow. Icarus, Vol. 252, pp. 144-149.

[2] E. Kaufmann, & A. Hagermann, 2017: Experimental investigation of insolation-driven dust ejection from Mars' CO2 ice caps. Icarus, Vol. 282, pp. 118-126.

[3] H. E. Chinnery et al.: The Penetration of Solar Radiation into Carbon Dioxide Ice. JGR Planets, in press.

[4] E. Kaufmann & A. Hagermann: Constraining the parameter space of comet simulation experiments. Icarus, Vol. 311, pp. 105-112.

[5] M. Grott et al.: The MASCOT Radiometer MARA for the Hayabusa 2 Mission. Space Sci Rev Vol. 208, pp. 413–431, 2017.

EPSC Abstracts
Vol. 12, EPSC2018-116, 2018
European Planetary Science Congress 2018

Reflectance spectra of solid organic acids and their mixtures with Fe-sulfide pyrrhotite: Insights into the surface composition of comet 67P/CG.

Xenia Meißner (1), **Lyuba Moroz** (2,3), Gabriele Arnold (3) and Klaus Rademann (1)
(1) Humboldt-Universität zu Berlin, Berlin, Germany (xenia.meissner@student.hu-berlin.de), (2) Universität Potsdam, Potsdam, Germany, (3) German Aerospace Center (DLR), Berlin, Germany

Abstract

We present 0.3-17 μm reflectance spectra of different solid organic acids (including amino acids) and their fine-grained intimate mixtures with pyrrhotite ($Fe_{1-x}S$), a Fe-sulfide. These data provide a valuable basis for compositional interpretation of remote sensing spectra of the comet 67P/CG's surface. In particular, we investigate the ability of an opaque Fe-sulfide to suppress absorption bands of organic acids and to modify key spectral parameters such as contrasts, widths, shapes of absorption bands and continuum slopes. Finally, we compare our results to the VIRTIS/Rosetta spectra of comet 67P surface in order to assess the possible contribution of carboxylic O-H vibrations to the broad complex 3.2-μm absorption band in the comet spectra.

1. Introduction

The Visible and InfraRed Thermal Imaging Spectrometer (VIRTIS) onboard Rosetta orbiter revealed that the surface of comet 67P/CG is dark from the near-UV to the IR and enriched in organic and opaque components [1,2]. The VIRTIS spectra of the 67P nucleus show a broad complex absorption feature around 3.2 μm consistent with the ubiquitous presence of a variety of organic components [2]. The broadness of the observed band can be explained by the contribution from carboxylic functional groups [1,2]. Fine-grained opaque phases (in particular the Fe-sulfides pyrrhotite or troilite) are likely responsible for the low IR reflectance and low contrast of the 3.2-μm absorption band [1,2]. The work by Istiqomah et al. [3] provided the first important steps towards understanding the possible contribution of carboxylic acids to the VIRTIS spectra of the 67P surface. Reflectance spectra of organic acids are barely available. Diagnostic absorption features of carboxylic acids can be strongly modified in the presence of intimately admixed opaque components [e.g., 4,5]. Thus, the evidence of carboxylic acids on the surface of 67P requires dedicated laboratory studies of laboratory analogs including opaque components.

2. Samples and Methods

We acquired a set of 23 solid organic acids containing carboxylic groups (including 6 amino acids) at the Department of Chemistry of the Humboldt-Universität zu Berlin. The choice of acids was not based on their particular relevance to cometary organics, but rather on their compositional diversity. In this study we were focused only on organic acids which are stable in a solid state at room temperature. Two types of acid powders were spectrally characterized – coarse-grained non-sorted powders and fine-grained powders manually ground in an agate mortar. Several selected organic acids were mechanically mixed in different proportions with a well-characterized [5] fine-grained (<25 μm) natural pyrrhotite. The mixtures were prepared by manual grinding of the mixed end-member powders in an agate mortar. Biconical reflectance spectra (0.3-17 μm) of pure acid powders and acid-pyrrhotite mixtures were measured at the Planetary Spectroscopy Laboratory (DLR, Berlin) in vacuum at i=e=15° or i=13°; e=17° using a Bruker VERTEX 80v FTIR-spectrometer equipped with a Bruker variable angle reflectance accessory.

3. Results

The measured reflectance spectra were analyzed in terms of key spectral parameters (positions, depths, widths and overall shapes of major absorption bands, continuum slopes, reflectance values). Particular attention was dedicated to the position and shape of the short-wavelength flank of the broad complex

feature around ~3.3 µm associated with carboxylic O-H stretching vibrations. Gradual changes of spectral parameters as a function of pyrrhotite content in the mixtures were investigated, quantified and compared to the corresponding parameters of the average spectrum of the 67P surface [6]. The results of the analysis will be presented and their implications for compositional interpretation of VIRTIS/Rosetta spectra will be discussed.

Acknowledgements

The samples of organic acids were kindly provided by Prof. Klaus Rademann from the Department of Chemistry of the Humboldt-Universität zu Berlin. We thank I. Büttner for assistance in sample preparation. L.M. acknowledges the DFG grant MO 3007/1-1.

References

[1] Capaccioni, F. et al.: Science, Vol. 347, 628, 2015.

[2] Quirico, E. et al.: Icarus, Vol. 272, 32-47, 2016.

[3] Istiqomah, I. et al.: EPSC Abstracts Vol. 11, EPSC2017-617, 2017.

[4] Moroz, L. and Arnold, G.: J. Geophys. Res. 104, E6, 14,109-14,122.

[5] Moroz, L.V. et al.: EPSC Abstracts Vol. 11, EPSC2017-266, 2017.

[6] Ciarniello, M. et al.: Astron. Astrophys. 583, A31.

EPSC Abstracts
Vol. 12, EPSC2018-152, 2018
European Planetary Science Congress 2018

Occurrence of graphite and sinoite in EL6 chondrites Eagle and Pillistfer

Noemi Mészárosová (1,2) and Roman Skála (1,2)
(1) The Czech Academy of Sciences, Institute of Geology, Rozvojová 269, CZ-165 00, Prague 6, Czech Republic (2) Institute of Geochemistry, Mineralogy and Mineral Resources, Faculty of Science, Charles University, Albertov 6, 128 43 Prague 2, Czech Republic; (meszarosova@gli.cas.cz)

1. Introduction

Enstatite chondrites are meteorites formed under highly reduced conditions and include two chemically distinct groups: EH (high bulk iron) and EL (low bulk iron) with petrological types ranging from 3 to 6 [10]. Classification for petrologic types developed by [9] and modified by later workers can be applied also for enstatite chondrites. Petrologic type 6 underwent high degree of thermal metamorphosis and is characterized beside other by poorly defined chondrules [6]; [7]. The reduced conditions of formation are reflected also in their mineralogy. They contain enstatite, Si bearing kamacite, Ti-Cr-bearing troilite, (Mg,Mn,Fe)-sulfides [solid solution including niningerite (MgS), alabandite (MnS) and keilite ($Fe_{>0.5}Mg_{<0.5}S$)] and oldhamite CaS ([10] and references therein). Recently, the study of enstatite chondrites has been focused on revealing their thermal history; especially on confirmation or disproving of shock melting processes ([1]; [2]; [7] and references therein).

2. Materials and methods

Fragments approximately 13 mm wide and 6 mm high of Eagle and Pillistfer meteorites were embedded into epoxy resin to produce polished sections. These were examined with reflected light microscopy and analytical scanning electron microscopy. Phase identification was performed by Raman microspectroscopy.

3. Results

Mineralogy of both meteorites is similar. No chondrules were observed in samples. Their matrix consists of mainly euhedral or subhedral grains with partially rounded edges of enstatite of almost pure end member composition with small amounts of CaO. Minor phase is plagioclase which occurs as irregular anhedral grains occasionally enclosing rounded grains of enstatite. Chemical composition is close to albite end member. Occasionally, silica-rich phase with minor amounts of Na, Al and Fe occurs along the grain boundaries of euhedral enstatite, plagioclase and/or metal/sulfide aggregates. Small (up to 10 μm) droplets of this silica-rich phase are also associated with metal and sulfide droplets. In addition to that, in Pillistfer, silica-rich phase forms some sort of dendritic structures with metal and schreibersite or sulfides. Silica-rich phases in both meteorites were identified as tridymite and cristobalite. Subhedral grains of sinoite appear in association with dendritic structures. In Eagle, sinoite occurs as subhedral grains in association with plagioclase and enstatite in matrix. Rarely, sinoite also appears as euhedral inclusion in troilite. Metal is Si-bearing kamacite (Si ~ 1 wt %; Ni < 6 wt % for both meteorites). Kamacite particles have irregular shapes partly rounded with embayed rounded enstatite grains in association with schreibersite and sulfides. In Eagle, kamacite rarely contains inclusions of more Ni rich parts (Ni up to 16 wt %). Kamacite in both meteorites contain inclusions of rounded grains of enstatite and graphite of various morphologies (feathery fan-shaped graphite, graphite chaplets or graphite booklets). Kamacite in Eagle contain more graphite inclusions than Pillistfer. In addition, in Eagle, graphite booklets also appear in silicate matrix. Edges of kamacite grains are slightly oxidized (this phenomenon is more obvious in Eagle, in which some thin veins of (Fe,Ni)-sulfate are observed along the grain boundaries of enstatite). Grain of FeSi was observed in kamacite few microns from such oxidized part. Sulfide minerals in both meteorites include Ti-Cr-bearing troilite (Ti < 1 wt % in both meteorites; Cr < 1 wt % in Eagle, Cr ~ 1 wt% in Pillistfer) with daubréelite exsolution lamellae and ferroan alabandite. In Pillistfer, oldhamite grains are also present.

4. Discussion

The presence of graphite and sinoite as well as euhedral enstatite grains have been presented as one of the possible indicators of impact melting ([4]; [5]; [7] and reference therein). However, temperature of formation of sinoite is similar to metamorphic temperatures expected for EL6 chondrites suggesting formation of sinoite over geologic timescale. The latter suggestion is also supported by the fact that sinoite amorphizes in dynamic events as was experimentally demonstrated by [8], which excludes the impact melting formation [1]. The silica-rich phase reported from other EL6 chondrites corresponds to either tridymite and/or cristobalite [3]. Based on very high stability temperature of cristobalite, which is close to temperatures of liquidus of enstatite chondrites, the formation of cristobalite from primordial EL6 material or derivation from chondrules is suggested. Survival of tridymite and/or cristobalite along the grain boundaries suggests crystallization from melt followed by fast cooling; similar textural context was observed in both studied EL6 meteorites. On the other hand, no shock textures were observed in these samples. Missing indication of shock compression may be due to thermal annealing of EL6 chondrites as was suggested already by [6].

5. Summary and Conclusions

Sole presence of sinoite, graphite and silica-rich phases do not provide an unambiguous evidence for any of the proposed mechanisms of the enstatite chondrite formation. The ultimate decision on the origin of these enigmatic meteorites would deserve more detailed study particularly that focused on isotopic character of graphite and sinoite as has already been demonstrated by [1]. Further, more detailed study focused on chemical composition of metal and sulfides should be carried out. The presented data on mineral chemistry does not seem to support the impact melting theory.

Acknowledgements

The research was supported within institutional support RVO 67985831 of the Institute of Geology of the Czech Academy of Sciences.

References

[1] El Goresy, A., Lin, Y., Miyahara, M., Gannoun, A., Boyet, M., Ohtani, E., Gillet, P., Trieloff, M., Simonovici, A., Feng, L. & Lemelle, L. (2017). Origin of EL3 chondrites: Evidence for variable C/O ratios during their course of formation—A state of the art scrutiny. Meteoritics and Planetary Science, 52(5), 781–806. https://doi.org/10.1111/maps.12832

[2] Horstmann, M., Humayun, M., & Bischoff, A. (2014). Clues to the origin of metal in Almahata Sitta EL and EH chondrites and implications for primitive E chondrite thermal histories. Geochimica et Cosmochimica Acta, 140, 720–744. https://doi.org/10.1016/j.gca.2014.04.041

[3] Kimura, M., Weisberg, M. K., Lin, Y., Suzuki, A., Ohtani, E., & Okazaki, R. (2005). Thermal history of the enstatite chondrites from silica polymorphs. Meteoritics and Planetary Science, 40(6), 855–868. https://doi.org/10.1111/j.1945-5100.2005.tb00159.x

[4] Rubin, A. E. (1997). Sinoite (Si2 N2O): Crystallization from EL chondrite impact melts. American Mineralogist, 82, 1001–1006.

[5] Rubin, A. E. (2015). Impact features of enstatite-rich meteorites. Chemie Der Erde - Geochemistry, 75(1), 1–28. https://doi.org/10.1016/j.chemer.2014.09.001

[6] Rubin, A. E., Scott, E. R. D., & Keil, K. (1997). Shock metamorphism of enstatite chondrites. Geochimica et Cosmochimica Acta, 61(4), 847–858. https://doi.org/10.1016/S0016-7037(96)00364-X

[7] Rubin, A. E., & Wasson, J. T. (2011). Shock effects in “EH6” enstatite chondrites and implications for collisional heating of the EH and EL parent asteroids. Geochimica et Cosmochimica Acta, 75(13), 3757–3780. https://doi.org/10.1016/j.gca.2011.04.002

[8] Sekine, T., He, H., Kobayashi, T., & Shibata, K. (2006). Sinoite (Si2N2O) shocked at pressures at 28 to 64 GPa. American Mineralogist, 91(2–3), 463–466. https://doi.org/10.2138/am.2006.2106

[9] Van Schmus, W. R., & Wood, J. A. (1967). A chemical-petrologic classification for the chondritic meteorites. Geochimica et Cosmochimica Acta, 31(5), 747–765. https://doi.org/10.1016/S0016-7037(67)80030-9

[10] Weyrauch, M., Horstmann, M., & Bischoff, A. (2018). Chemical variations of sulfides and metal in enstatite chondrites—Introduction of a new classification scheme. Meteoritics and Planetary Science, 53(3), 394–415. https://doi.org/10.1111/maps.13025

EPSC Abstracts
Vol. 12, EPSC2018-179, 2018
European Planetary Science Congress 2018

Laboratory developments to support space missions exploring the Solar System

N. Abou Mrad (Belles-Limeul), A. Fresneau, F. Duvernay, L. d'Hendecourt, **G. Danger**
Aix-Marseille Université, CNRS, PIIM, UMR 7345, 13013 Marseille, France (gregoire.danger@univ-amu.fr / website: http://piim.univ-amu.fr/Equipe-ASTRO)

Abstract

All our approaches shows that laboratory simulation provides important information on the analysis of data coming from space missions (eg Rosetta). They are also useful in the preparation of future space missions either for determining the environments where such missions can be performed, or for giving information for the definition and the development of analytical tools of these missions. The last impact of laboratory simulation consists in testing these analytical tools before their shipping. By taking example of what we are developing in our laboratory, we will discuss about the different interests that could emerge by developing a close collaboration between ground experiments and space mission development laboratories.

1. Introduction

Understanding of the evolution of organic matter in astrophysical environments is a important field of research in astrobiology. It provides clues about its composition and on its availability throughout the Universe for leading ultimately in some environments to chemical systems which may precede the emergence of biochemical systems. For understanding this evolution , several approaches can be considered. The first approach consists in observing the different astrophysical environments from telescopes or satellites. These observations allow to get important information on physical and chemical processes that can occur in environments observed as well as on the understanding of the evolution of these objects. However, the information about the chemical evolution in these environments is restricted to simple chemical systems having only few atoms. For obtaining more information on the evolution of more complex chemical systems, another approach is the analysis of Solar system objects such as comets, asteroids, meteorites or planets. This can be done by in situ space missions whose objective is to meet (or even contact) some of these objects and analyze their composition (Rosetta space mission , Mission Hayabus , Mission Martian Curiosity , Cassini - Huygens mission). Characterizations of such object can also be performed by using sophisticated analytical methods on Earth as for meteorites or sample return. All these observational data allows us to compare different states of the natural organic matter and establish a first evolution of this material. However, they do not allow to trace the overall evolution of this material without the use of specific tracers of molecular evolution. That is why a complementary approach is the development of terrestrial experimental systems for simulating astrophysical environments. The interest of these simulations is to study simple systems (bottom-up approach describing the successive steps of molecular evolution) as well as complex systems (top-down approach, which consists in providing a refined description of extraterrestrial material analog). These simulations are used for example for understanding the evolution of the organic matter from interstellar grains to its incorporation within Solar system objects such as comets.

2. Implications of experimental simulation for space exploration

We believe that beyond the essential information that provide laboratory simulations for understanding the evolution of organic matter in astrophysical environments, experimental simulation can and must play an essential role in the development of instrumentations for future space exploration as well as data processing and data interpretation obtained from these space missions. Laboratory simulations may indeed have an essential impact in different stages (in chronological terms) of space programs through the points below:

1 - Refine the choice of environments in which space missions must be carried out,
2 - Prepare the development of analytical devices,

3 - Test and qualify prototypes of space missions,
4 - Limit the risks associated with these missions,
5 - Develop and validate tools for analyzing data from space missions,
6 - Optimizing scientific return of space missions.

3. An example of experimental simulation

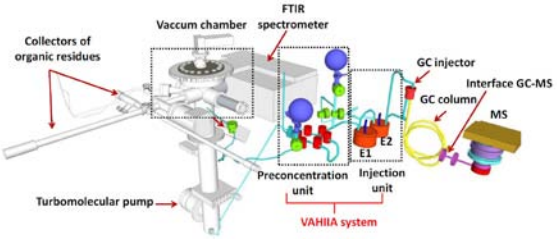

The AHIIA system allowing to simulate the evolution of astrophysical ices and identification and quantification of organic molecules formed.

Our group develops experimental simulations for investigating the chemical reactivity and the chemical evolution that occur during star formation or in cometary environments. We develop two complementary approaches.
Next to a bottom-up approach, which consists in studying the reactivity that can lead to the formation of molecules in astrophysical environments, we are developing a top-down approach. In this case, we investigate the overall evolution of the organic matter in astrophysical environments and not anymore specific reactions. The first project consists in analyzing the whole compounds that sublime during the warming of a cometary ice analog[1–3]. This approach will give us important information of volatile molecules that could be detected in the gas phase of a particular object, and should thus improve the understanding of observations. Another approach consists in analyzing the whole residue that is formed after the warming of an ice analog. In this case, our aim is to find the best analytical method for obtaining whole information of the evolution of these analogs. The aim is to obtain a mapping of this evolution that could then be compared to astrophysical objects such as meteorites. We currently focus our investigation on high resolution mass spectrometry associated to the development of specific data treatment [4–6]. The protocols developed can be then used for future space missions using high resolution mass spectrometry (e.g. orbitrap) as well as for the analyses of astrophysical objects on ground base. During this presentation, we will present the last developments and results obtained from the AHIIA systems.

Acknowledgements

This work has been funded by the French national programme "Physique Chimie du Milieu Interstellaire" (P.C.M.I, INSU), “Programme National de Planétologie” (PNP, INSU), "Environnements Planétaires et Origines de la Vie" (EPOV, CNRS), the "Centre National d’Études Spatiales" (C.N.E.S) from its exobiology program and by the "Agence Nationale de la Recherche" through the ANR-VAHIIA (ANR-12-JS08-0001-01) and RAHIIA_SSOM (ANR-16-CE29-0015).

References

1 N. Abou Mrad, F. Duvernay, P. Theulé, T. Chiavassa and G. Danger, Development and optimization of an analytical system for volatile organic compound analysis coming from the heating of interstellar/cometary ice analogues, *Anal. Chem.*, 2014, **86**, 8391–9.

2 N. Abou Mrad, F. Duvernay, T. Chiavassa and G. Danger, Methanol ice VUV photo- processing: GC-MS analysis of volatile organic compounds, *Mon. Not. R. Astron. Soc.*, 2016, **458**, 1234.

3 N. Abou Mrad, F. Duvernay, R. Isnard, T. Chiavassa and G. Danger, The gaseous phase as a probe of the astrophysical solid phase chemistry, *Astrophys. J.*

4 G. Danger, F. Orthous-Daunay, P. de Marcellus, P. Modica, V. Vuitton, F. Duvernay, L. Flandinet, L. Le Sergeant d’Hendecourt, R. Thissen and T. Chiavassa, Characterization of laboratory analogs of interstellar/cometary organic residues using very high resolution mass spectrometry, *Geochim. Cosmochim. Acta*, 2013, **118**, 184–201.

5 G. Danger, A. Fresneau, N. Abou Mrad, P. de Marcellus, F. Orthous-Daunay, F. Duvernay, V. Vuitton, L. Le Sergeant d’Hendecourt, R. Thissen and T. Chiavassa, Insight into the molecular composition of laboratory organic residues produced from interstellar/pre-cometary ice analogues using very high resolution mass spectrometry, *Geochim. Cosmochim. Acta*, 2016, **189**, 184–196.

6 A. Fresneau, N. A. Mrad, L. LS d’Hendecourt, F. Duvernay, L. Flandinet, F.-R. Orthous-Daunay, V. Vuitton, R. Thissen, T. Chiavassa and G. Danger, Cometary Materials Originating from Interstellar Ices: Clues from Laboratory Experiments, *Astrophys. J.*, 2017, **837**, 168.

EPSC Abstracts
Vol. 12, EPSC2018-284, 2018
European Planetary Science Congress 2018

Space weathering in enstatite single crystals: Femtosecond laser pulse experiments simulate micrometeoroid impacts

Doreen Schmidt (1), Kilian Pollok (1), Gabor Matthäus (2), Harald Mutschke (3), Stefan Nolte (2) and Falko Langenhorst (1)
(1) Institute of Geosciences, Friedrich Schiller University (FSU), Carl-Zeiss-Promenade 10, 07745 Jena, Germany (2) Institute of Applied Physics (IAP), FSU, Albert-Einstein-Str. 15, 07745 Jena, Germany (3) Astrophysical Institute and University Observatory (AIU), FSU, Schillergässchen 2-3, Jena 07745, Germany (doreen.turner@uni-jena.de)

Abstract

Oriented slices of enstatite single crystals were irradiated by femtosecond laser pulses. Reflectance spectra of the irradiated surfaces show distinct darkening compared to the unprocessed surfaces as a typical feature of space weathered material. The microcraters contain a glass layer at the surface, but there is no formation of iron nanoparticles. The crater surfaces show different fracturing depending on their orientation. Also, the microstructures in the depth of the craters and therefore the deformation mechanisms differ according to the orientation.

1. Introduction

Space weathering, occurring on airless bodies in the solar system, alters the surfaces of planetary materials by micrometeoroid bombardment and solar wind irradiation. The effects of space weathering are responsible for the differences in reflectance spectra between pristine and weathered planetary materials such as darkening and reddening [1]. Pulsed laser experiments are known to reproduce space weathering effects on olivine like melting, the formation of iron nanoparticles and deformation features like dislocations [2] as well as other planar shock effects [3]. Comparable observations are made on natural olivines in lunar or asteroidal samples [4,5]. In this context we pursued further laser experiments on pyroxene, which is besides olivine one of the most important planetary minerals.

2. Material and Methods

Kilosa enstatite containing about 4 wt% Fe (En_{93}) was cut perpendicular to the crystallographic axes, i.e. parallel to the (100), (010) and (001) planes. Additionally, samples were prepared parallel to the (210), (211) and (301) planes. The samples were sliced plane-parallel to a thickness between 0.5 and 1.0 mm and double sided polished.

Laser irradiation was performed on the polished surfaces under vacuum (10^{-3} mbar) using a Ti:sapphire laser at 800 nm wavelength. Each pulse had a spot size of 38 µm ($1/e^2$) and a duration of 100 fs. We used a laser energy of 3 mJ resulting in a laser intensity of 10^{15} W/cm^2. This reproduces well the spatial and temporal conditions of natural micrometeoroid impacts. 20 x 20 shots were executed with a spacing of 100 µm to produce a grid with an irradiated area of 2 mm^2.

NUV-VIS-NIR spectral measurements were performed in reflectance at near-normal incidence with a Perkin Elmer Lambda 19 spectrometer. The spectral range of 200-2,500 nm was measured with a scan speed of 120 nm/min and a 1 nm step size. The acquired spectra were corrected with respect to a calibrated aluminum mirror.

The recovered material was investigated with SEM (FEI Quanta3D FEG) and TEM (FEI Tecnai G 2 FEG). Sample preparation for TEM was done with focused ion beam (FIB) technique by cutting 100 nm thin lamellae perpendicular to the irradiated surface.

3. Results

3.1 Surface Analysis of the Microcraters

The laser single shots produced mainly spherical to partly irregularly shaped microcraters with a distinct splash-like layer. There are different amounts of radially ejected material. The samples parallel to (001) and (210) show strong fracturing at the crater surfaces, subordinately also the (100) cut sample. The craters produced on the (001) plane have cracks mainly subparallel to the traces of the cleavage

planes on {210} and (100) with smaller subspherical cracks at the crater rim. The fractures of the (210) sample show a preferred orientation parallel to the [001] direction, whereas the (100) sample is fractured mainly subparallel to [010] and [001]. There are no fractures at the crater surfaces of the samples parallel to the (010), (301) and (211).

3.2 Spectroscopy

Reflectance spectra of the processed samples show a decrease in intensity with respect to the unprocessed surfaces. This is known as spectral darkening. If the reflectance at longer NIR wavelengths is less reduced than in the shorter UV-VIS range, the spectrum gets redder. This effect is observed in most samples, but the intensity of reddening varies strongly between the differently orientated samples.

3.3 Microstructures

TEM investigations of the craters reveal a layered structure independent of the sample orientation. From top to bottom there is a glass layer, a dominant mechanically deformed layer containing shock defects and the undeformed substrate. All samples show parallel planar lamellae, that are amorphous in the upper part of the deformed layer and become thinner towards the bottom until they turn to microfractures or stacking faults. At the interface to the glass layer there are always two conjugated directions of the amorphous features, which have an angle of 30-50° to the surface normal. Deeper in the deformed layer the samples have either domains with subparallel lamellae in different orientations, or the layer contains homogeneously lamellae with one dominant or two conjugated directions. Activated cleavage planes can only be observed in the (210) sample, where the lamellae are parallel to the (100) cleavage. The transformation to clinoenstatite can be seen in the (301) sample. It occurs in the lower part of the deformed layer associated with microfractures and dislocations.

4. Discussion

The main deformation features in our shocked enstatite are microfractures and lamellae that probably represent shear planes. Frictional heating along these shear planes leads to amorphization. These experimentally produced structures are in good agreement with observations in natural samples like the Martian Meteorite Allan Hills 84001 [6]. We did not observe the formation of iron nanoparticles, which are generally regarded to be the main cause for the spectral darkening and reddening in naturally space weathered pyroxene [5] or have been observed in other experimentally irradiated pyroxene powder pellets [7].

Acknowledgements

We thank the DFG for support within the Leibniz program (LA830/14-1) and the research unit FOR 2285 “Debris Disk in Planetary Systems” (LA830/20-1).

References

[1] Bennett, C. J. et al.: Space-Weathering of Solar System Bodies: A Laboratory Perspective, Chemical reviews 113:9086–9150, 2013.

[2] Fazio, A. et al.: Femtosecond laser irradiation of olivine single crystals: Experimental simulation of space weathering, Icarus 299:240–252, 2018.

[3] Seydoux-Guillaume, A.-M. et al.: Dominance of mechanical over thermally induced damage during femtosecond laser ablation of monazite, European Journal of Mineralogy 22:235-244, 2010.

[4] Noble, S. K. et al.: The Microstructure of a Micrometeorite Impact into Lunar Olivine, Space Weathering of Airless Bodies: An Integration of Remote Sensing Data, Laboratory Experiments and Sample Analysis Workshop, Houston, USA, 2-4 November 2015, LPI Contribution No. 1878, Abstract 2034.

[5] Noguchi T. et al.: Space weathered rims found on the surfaces of the Itokawa dust particles, Meteoritics & Planetary Science 49:188-214, 2014.

[6] Barber, D.J. and Scott, E.R.D.: Shock and thermal history of Martian meteorite Allan Hills 84001 from transmission electron microscopy, Meteoritics & Planetary Science 41: 643-662, 2006.

[7] Nakamura, K. et al.: Laboratory Simulation of Space Weathering: Comparison Study of Microstructures of the Laser Irradiated Olivine and Pyroxene, 65th Annual Meeting of the Meteoritical Society, Los Angeles, USA, 21-26 July 2002, Abstract 5186.

EPSC Abstracts
Vol. 12, EPSC2018-308, 2018
European Planetary Science Congress 2018

The tensile strength of ice and dust aggregates

Christopher Kreuzig (1), Bastian Gundlach (1), Dorothea Bischoff (1), Stephan Kothe (1), Farangis Rezaei (1,3), Kim Paul Schmidt (2), Jürgen Blum (1), Benjamin Grzesik (3) and Enrico Stoll (3)
(1) Institut für Geophysik und extraterrestrische Physik, Technische Universität Braunschweig
(2) Institut für Physik der Kondensierten Materie, Technische Universität Braunschweig
(3) Institut für Raumfahrtsysteme, Technische Universität Braunschweig

Abstract

In order to understand the early formation of planets in the solar system and the activity of comets the tensile strength of astrophysical materials is of major importance. Therefore we currently developed a method to measure the tensile strength of ice and dust aggregates. The measured tensile strength for dust aggregates is depending on the grain size and for water ice it is very low compared to the theoretical predictions, so the specific surface energy has to be an steep function of temperature and very low at 150K.

1. Introduction

The tensile strength describes the maximum mechanical force a material can resist before it breaks. The knowledge of this parameter is important in astrophysics, because it describes the mechanical behaviour. In the formation of planets, the kilometre-sized planetesimals were formed by collisions of millimetre-sized aggregates. These were grown out of micrometre-sized particles, also by collisions. Besides other physical parameters, the tensile strength influences the growth of particles. [4].
For comets, the tensile strength is also very important to describe the dust activity [5]. The reason for the activity is the sublimation of icy materials, mainly water ice. The resulting gas pressure can eject aggregates from the surface by momentum transfer, if it is sufficient to overcome the tensile strength of the aggregate packing. In this picture, the presence of millimetre-sized particles in the coma can be explained, but not the existence of smaller micrometre-sized particles. For their existence, the aggregates must be broken by an unknown mechanism, which must provide a disruption stress greater than the tensile strength.
Motivated by this importance, an experiment was designed to measure the tensile strength of ice and dust aggregates.

2. The experiment

For this purpose the Brazilian Disc Test was chosen. This method uses a piston is used to compress a cylindrical sample (disc) until it fails. The maximum force is measured and used to calculate the tensile strength [1]. The experimental setup is shown in figure 1. The tensile strength σ is than calculated by

$$\sigma = \frac{2\,F}{\pi\,l\,d} \tag{1}$$

where F is the maximum force, d the diameter and l the thickness of the disc.
The samples were formed in a press, so that the diameters of all dust and ice samples were the same value. The thickness is determined by the amount of material used and was typically $11 - 26mm$. For the compression of the samples we used always the same pressure to achieve a constant volume filling factor.
To be able to perform measurements with ice the whole experiment was cooled with liquid nitrogen. Because the discs were very fragile and the temperature had to be very low (less than 150K), the experiment were performed directly inside the press without touching or moving the disk. The temperature of all parts in contact with the sample and the air around it were measured to ensure no sintering happens, so the temperature is always under 150K ([2] for details).
The exerted force was measured by a scale underneath the sample and the resulting cracks were observed by a camera.

3. Results

In figure 2, a typical measured curve is shown. In the first 40 seconds, the piston is moving without touching the sample, thus, the scale measures zero force. Therefore the tensile strength calculated with equation 1 is also zero. When the force starts to rise, the piston touches the sample. The maximum force is measured

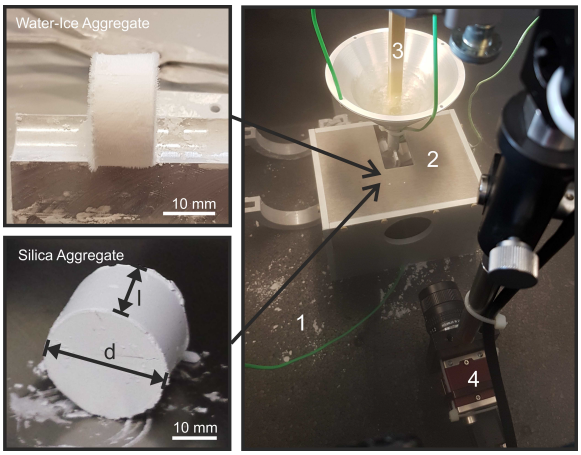

Figure 1: Images of the aggregates (left) and the experimental setup (right) used. Components visible in the image: styrofoam box (1) and metal housing (2) needed for low temperatures, piston (3) controlled by a stepper motor to exert pressure and the camera (4) to observe the crack appearing. The scale required for monitoring the exerted force is positioned underneath the styrofoam box and so not visible in the image [3].

at the point of breakup. After that, the force is depending on the crack, but not important for the tensile strength.
The tensile strength of the dust samples depends on the size of the particles used, so it gets higher with smaller particles.
Due to the extreme fragility of the ice samples the measured tensile strength is very low, even in regard of the bigger particle sizes. The tensile strength is $1.2 \pm 0.6 kPa$ with a volume filling factor of $\Phi = 0.5$. This value is less than the expected tensile strength for dust at this grain size, so the surface energy of water ice at 150K must be much lower than expected, so it is a steep function of temperature.

4. Summary and Conclusions

In this work the principal of the Brazilian Disk Test was used to measure the tensile strength of ice and dust samples. Therefore the experiment was modified to enable low temperatures. The results show, that the tensile strength of water ice below 150K is much smaller than expected, so the surface energy must be much smaller at these temperatures than previously assumed. This means for astrophysical models that ice cannot be used as glue for the aggregates in the formation of planets.

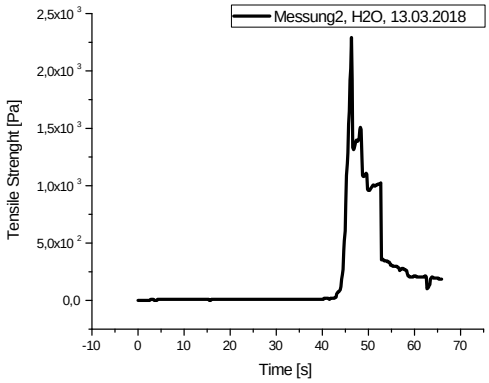

Figure 2: Example for a typical tensile strength measurement of an ice aggregate. With the force measured by the scale, the tensile strength was calculated by using equation 1. The temporal evaluation of the tensile strength is shown. During the experiment the temperatures were always under 150K. The maximal tensile strength measured is used for every sample.

Acknowledgements

We thank the DFG (BL 298/22-1 and BL 298/24-1) and the DLR (50 WM 1536) for supporting this project.

References

[1] Diyuan L., Wong L. N. Y.: The Brazilian Disc Test for Rock Mechanics Applications: Review and New Insights, Rock Mechanics and Rock Engineering, 46, 269, 2013

[2] Gundlach B., Ratte J., Blum J., Oesert J., Gorb S. N.: Sintering of micrometer-sized water-ice particles and the formation of surface crusts on icy Solar System bodies, Submitted to MNRAS, 2018

[3] B. Gundlach, K. P. Schmidt, C. Kreuzig, D. Bischo, F. Rezaei, S. Kothe, J. Blum, B. Grzesik, E. Stoll: The tensile strength of ice and dust aggregates and its dependence on particle properties, Submitted to MNRAS, 2018

[4] Güttler C., Blum J., Zsom A., Ormel C., Dullemond C. P.: Numerical simulations of highly porous dust aggregates in the low-velocity collision regime, Astronomy and Astrophysics, 513, A56, 2010

[5] Kuehrt E., Keller H. U., Icarus: Meteorites, The formation of cometary surface crusts, 109, 121, 1994

EPSC Abstracts
Vol. 12, EPSC2018-333, 2018
European Planetary Science Congress 2018

Analysis of reflectance spectra of enstatite-oldhamite mixtures for comparison with 2867 Šteins

Kathrin Markus (1), Gabriele Arnold (2), Lyuba Moroz (3,2), Daniela Henckel (2,4), and Harald Hiesinger (1)
(1) Institut für Planetologie, Westfälische Wilhelms-Universität Münster, Germany (kathrin.markus@uni-muenster.de), (2) DLR, Institut für Planetenforschung, Berlin, Germany, (3) Institut für Erd- und Umweltwissenschaften, Universität Potsdam, Germany, (4) Institut für Geologische Wissenschaften, Freie Universität Berlin, Germany.

Abstract

We present 0.3-17 µm reflectance spectra of synthetic orthoenstatite ($Mg_2Si_2O_6$), synthetic oldhamite (CaS), and their mixtures that can be used as analogue materials for comparison with E[II]-type asteroids like 2867 Šteins. We investigate the spectral behavior of the mixtures in regard to their oldhamite content and especially the changes in band depth in the VIS.

1. Introduction

2867 Šteins is a main belt asteroid and was discovered in 1969 [1]. It was a fly-by target of ESA's Rosetta mission in 2008 [2] and was previously studied with ground-based observations (e.g., [3,4,5,6,7,8]). It was classified as an E[II]-type asteroid [3]. E-type asteroids are characterized by high geometric albedos and flat or slightly reddish and featureless VIS and NIR reflectance spectra and are generally linked to the enstatite achondrites aubrites [9]. The E[II]-subtype asteroids show a strong absorption band at ~0.49 µm, and sometimes a weaker band at ~0.96 µm [10]. These absorption bands are attributed to oldhamite [11]. However, oldhamite usually only occurs as an accessory mineral in aubrites [12] while the required abundance of oldhamite needed to reproduce the absorption band in mathematical model mixtures is much higher (>40%) [4,5]. As a member of the E[II]-type asteroids, Šteins shows these absorptions bands. The depth of the absorption band at 0.49 µm is reported to be 9-13 % [4,6,7,8]. We present laboratory reflectance spectra of mixtures between synthetic orthoenstatite [13] and synthetic oldhamite for the comparison with reflectance spectra of Šteins and discuss the changes in the strength of the visible absorption band in relation to the oldhamite content of the mixtures.

2. Laboratory measurements

We collected biconical reflectance spectra from 0.3 to 17 µm of mixtures of synthetic orthoenstatite and oldhamite. All spectra were measured in vacuum using a Bruker Vertex VERTEX 80v FTIR-spectrometer at the Planetary Spectroscopy Laboratory (PSL) of the Institute of Planetary Research at DLR, Berlin. The same setup as in [13] was used. The orthoenstatite sample was synthesized and characterized in [13]. The composition of the sample is $En_{99.9}Fs_{0.03}Wo_{0.0}$ [13]. The oldhamite sample was obtained as synthetic calcium sulfide (99.95 %, CAS #20548-54-3) from abcr GmbH. We verified our CaS sample being crystalline oldhamite by using XRPD at the Institute for Mineralogy at the University Münster. Mixtures of the two endmembers were produced in 10 vol% steps with additional mixtures with 5, 3, and 1 vol% oldhamite. The weighted sample materials for each mixture were mechanically mixed for at least 30 minutes.

3. Reflectance spectra

The oldhamite spectrum shows a major absorption band at 0.41 µm. The depth of the absorption band is 6.0 % relative to a fitted linear continuum and calculated as the difference between the reflectance of the continuum and the spectrum at the band minimum. The spectrum is characterized by the red continuum slope throughout the near UV and visible ranges. Spectra from 0.3-1 µm of the endmembers and the mixtures are shown in Figure 1. The depth of the absorption band decreases with decreasing amount of oldhamite in the mixtures (Fig. 2). At oldhamite contents <20 vol% the depth of the absorption bands changes rapidly while the change is much slower at oldhamite contents between 20 and 100 vol%.

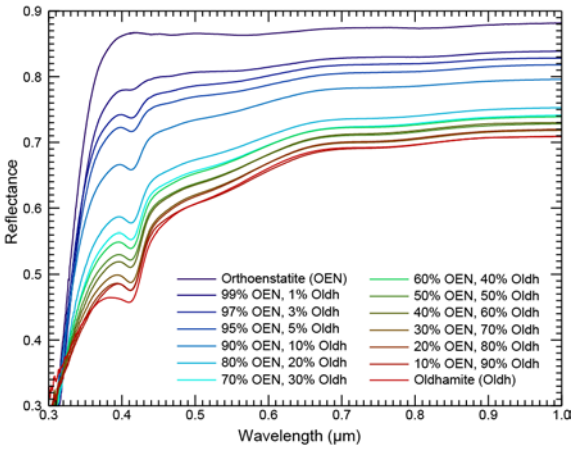

Figure 1: Reflectance spectra of orthoenstatite, oldhamite, and their mixtures from 0.3 to1 µm. Composition of mixtures is given in vol%.

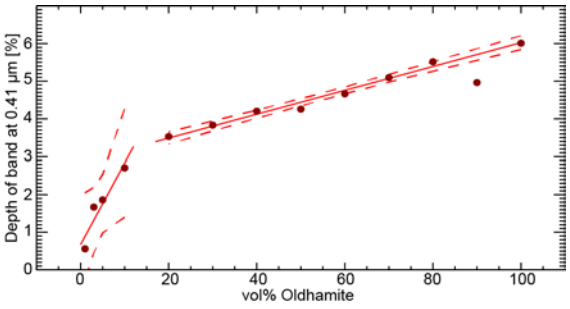

Figure 2: Depth of the absorption band at 0.41 µm. Linear fits are displayed as a continuous line. 2σ uncertainties of the fits are shown as dashed lines. The value at 90 vol% oldhamite has been excluded from the fit as an outlier.

In the MIR the oldhamite spectrum shows a much higher overall reflectance than the orthoenstatite and several broad absorption bands (e.g., between 6 µm and 7.4 µm and at 8.9 µm and 10.5 µm). A very narrow absorption band is visible at 6.59 µm. The detailed description of the orthoenstatite spectral features is provided in [13]. The spectra of the mixtures with 1, 2, 5, and 10 vol% of oldhamite are almost identical to the orthoenstatite spectrum, especially in the Reststrahlen bands. The spectra of mixtures with ≥20 vol% oldhamite show a significant increase in overall reflectance. The absorption band at 6.59 µm is clearly visible in all spectra of mixtures with ≥20 vol% oldhamite. In the spectra of the mixtures with 10 vol%, 5 vol%, and 3 vol% oldhamite it is only visible as a weak feature.

4. Conclusion

Our laboratory measurements of synthetic oldhamite does not show the absorption band at 0.49 µm observed in E[II]-type asteroids and oldhamite picked from the aubrite Norton County [11]. Instead, our spectra show an absorption band at 0.41 µm, which was previously also reported in [14]. Therefore, the spectra of our mixtures do not enable us to constrain the oldhamite abundance needed to reproduce the absorption band observed in Šteins' spectra. However, our data on the depth of the absorption band at 0.41 µm shows, that the depths does not follow a simple linear trend. [4] and [5] used areal (linear) mixing models for their estimates of the composition of Šteins. A linear trend would overestimate the required abundance of oldhamite for a given band depth. In the MIR our spectra show that oldhamite contents <20 vol% do not alter the spectral features typical for enstatite.

References

[1] IAU Minor Planet Center: www.minorplanetcenter.net/iau/lists/NumberedMPs000001.html, Last updated: 04.05.2018

[2] Keller, H.U. et al.: Science 327, 190-193, 2010.

[3] Barucci, M.A. et al.: Astronomy & Astrophysics 430, 313-317, 2005.

[4] Nedelcu, D.A. et al.: Astronomy & Astrophysics 473, L33-L36, 2007.

[5] Dotto, E. et al.: Astronomy & Astrophysics 494, L29-L32, 2009.

[6] Fornasier, S. et al.: Astronomy & Astrophysics 474, L29-L32, 2007.

[7] Fornasier, S. et al.: Icarus 196, 119-134, 2008.

[8] Weissman, P.R et al.: Meteoritics & Planetary Science 43, 905-914, 2008.

[9] Gaffey, M.J. et al.: Meteoritics 28, 161-187, 1993.

[10] Gaffey, M.J., Kelley, M.S.: Lunar and Planetary Science Conference XXXV #1812, 2004.

[11] Burbine, T.H. et al.: Meteoritics & Planetary Science 37, 1233-1244, 2002.

[12] Keil, K.: Chemie der Erde - Geochemistry 70, 295-317, 2010.

[13] Markus, K. et al.: Planetary and Space Science, In Press, 2018.

[14] Izawa, M.R.M. et al.: Icarus, 226, 1612-1617, 2013.

EPSC Abstracts
Vol. 12, EPSC2018-385, 2018
European Planetary Science Congress 2018

2D and 3D FTIR hyperspectral imaging of the Paris meteorite

Z. Dionnet (1,2), F. Borondics (2), A. Aléon-Toppani (1), D. Baklouti (1), F. Brisset (3), Z. Djouadi (1), A. King (2), C. Sandt (2), D. Troadec (4) and **R. Brunetto** (1)

(1) Institut d'Astrophysique Spatiale, CNRS, Université Paris-Saclay, Orsay, France, (2) Synchrotron SOLEIL, Saint-Aubin, France, (3) Institut de Chimie Moléculaire et des Matériaux d'Orsay, Université Paris-Saclay, Orsay, France, (4) Institut d'Electronique, de Microélectronique et de Nanotechnologie, Lille, France (rosario.brunetto@ias.u-psud.fr)

Abstract

Significant compositional and structural heterogeneity at nm to mm scales is an important characteristic of primitive extraterrestrial materials. This heterogeneity has been observed by different techniques such as infrared (IR) micro spectroscopy mapping which is a powerful tool as it is (a) non-destructive, (b) allows comparison with astronomical observations of primitive Solar System small bodies (asteroids, comets) [1] and (c) access both to the mineral and carbonaceous phases. It also allows hyperspectral imaging studies, useful to visualize the spatial distribution of different components, their assembly and thus to deduce constraints about their formation and their evolution in the young Solar System.

Here, we report the analysis of high-resolution Fourier Transform IR hyperspectral imaging analytical measurements at the micron scale on a fragment of the Paris meteorite (one of the most primitive carbonaceous chondrites [2]), supported by Raman and SEM-EDS measurements. The fragment is crushed in a diamond compression cell. The micro-FTIR analyses are performed in transmission with two setups, an imaging microscope with a matrix detector using a thermal source and a system using a single point detector coupled with the synchrotron source at the SOLEIL synchrotron facility (SMIS beamline).

We obtain the spatial distribution of chemical/mineralogical components. We confirm at a larger scale (10 μm) the presence of hydrated amorphous silicates observed at a smaller scale (1 μm). Based on the relative abundance of different minerals (hydrated amorphous silicate, olivine, diopside and serpentine) we propose a sequence of aqueous alteration. Considering the spatial correlation of minerals with organic matter, we discuss the effects of aqueous alteration on the organic matter in bulk. In particular, we detect an increase of the CH2/CH3 ratio in the altered zone and present the possible scenarios that lead to the observed chain length shortening/cracking of hydrocarbons [3].

Thanks to the Focal Plane Array detector, 3D hyperspectral micro-tomography can be performed to access structural information on intact samples [4]. Here, we also present the first 3D infrared reconstruction of three fragments of the Paris meteorites combined to X-ray micro-tomography. Using a Focused Ion Beam (FIB), we fix the samples at the extremity of a needle (Fig. 1). This preparation minimizes the organic contamination. Then we perform IR 3D hyperspectral micro-tomography at SMIS to reconstruct the sample at different wavelengths and to reconstruct the spatial distribution of the different components. This allows to study the 3D spatial correlation between the meteoritic organic and mineral phases at scales down to ~3 μm.

Moreover, X-rays tomography is also performed on the same Paris particles (see Figure 1(c)), at the PSICHE beamline of the synchrotron SOLEIL, to obtain complementary information about the physical properties of the grains (shape, fractures, porosity). X-ray analysis are performed at low energy to preserve the organic matter inside our sample. By combining X-ray and FTIR data we obtain a physico-chemical description of precious grains in a non-destructive way.

Performing FTIR micro-tomography on extraterrestrial samples rich in organic matter, is an important step in view of the sample return of dust particles from carbonaceous asteroids Ryugu by the

Hayabusa2 mission and Bennu by OSIRIS-REx mission. In the sequence of analyses, micro-FTIR 3D spectral imaging coupled with X-rays tomography can provide a first, powerful non-destructive characterization of whole grains, in order to identify areas of interest and provide useful information before subsequent destructive analyses.

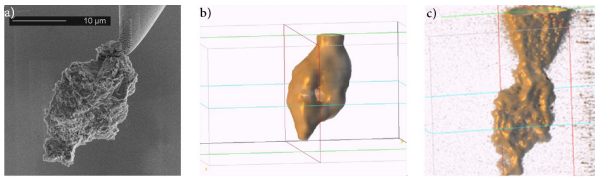

Figure 1: Paris meteorite sample welded at the extremity of the tungsten needle thanks to FIB preparation (a) TEM image, (b) IR reconstruction of the continuum at 2.6 µm and (c) X-ray reconstruction at 20 keV.

Acknowledgements

This work is supported by the "IDI 2015" project funded by the IDEX Paris-Saclay (Grant ANR-11-IDEX-0003-02), and funded by the French national program “Programme National de Planetologie” (PNP) and by the ANR project RAHIIA_SSOM (Grant ANR-16-CE29-0015-01) of the French Agence Nationale de la Recherche. The microspectroscopy activities are supported by grants from Région Ile-de-France (DIM-ACAV) and SOLEIL. We thank E. Boulard, L. d’Hendecourt, E. Quirico, and B. Zanda for fruitful discussions, and P. Beck and Y. Kebukawa for providing IR data of meteorites.

References

[1] Brunetto, R., and 10 colleagues: Mid-IR, Far-IR, Raman micro-spectroscopy, and FESEM-EDX study of IDP L2021C5: Clues to its origin, Icarus, Vol. 212, pp. 896-910, 2011.

[2] Hewins, R.H., and 16 colleagues: The Paris meteorite, the least altered CM chondrite so far, Geochimica et Cosmochimica Acta, Vol. 124, pp. 190-222, 2014.

[3] Dionnet, Z., Aleon-Toppani, A., Baklouti, D., Borondics, F., Brisset, F., Djouadi, Z., Sandt, C., and Brunetto, R.: Organic and mineralogic heterogeneity of the Paris meteorite followed by FTIR hyperspectral imaging, Meteoritics and Planetary Science, 2018 submitted.

[4] Martin M.C., and 12 colleagues: 3D spectral imaging with synchrotron Fourier transform infrared spectro-microtomography, Nature Methods, Vol. 10, pp. 861–864, 2015.

EPSC Abstracts
Vol. 12, EPSC2018-412, 2018
European Planetary Science Congress 2018

Comet simulation experiments – a simplified approach

Erika Kaufmann and Axel Hagermann
Department of Biological and Environmental Sciences, University of Stirling (erika.kaufmann@stir.ac.uk)

Abstract

Rosetta and other cometary missions have returned data that are interpreted based on predictions of theoretical models and the results of laboratory experiments (e.g. [1]). Our work supports Rosetta's observations by investigating the influence of insolation on the hardening process of the near-surface layers and the change in surface morphology. Our sample consists of pure, porous H_2O ice and carbon black particles. The final results of our experiments suggest that translucence of the near-surface ice is an important factor in the process of subsurface hardening. Our experiments also produced large, low-density dust aggregates from pure carbon particles on the sample surface.

1. Introduction

Our knowledge about the physical processes of comets is based on data from several space missions (most recently ROSETTA), the predictions of theoretical models and the results of laboratory experiments.
A number of comet simulation experiments performed in the past (e.g. KOSI [2]) have deepened our understanding of the physics that drives cometary activity and alters cometary nuclei. Although those experiments improved the understanding of the physics and morphology of cometary analogue materials, for most of them the set-up was quite complex and made it difficult to analyse the results in a quantitative manner.
In order to avoid these difficulties we decided to start a series of experiments using samples that only contain two components – H_2O ice and carbon particles (carbon black).

2. Experiments

To investigate the influence of subsurface solar light absorption by dust, we added varying quantities of carbon particles to samples of porous ice (0.02% to 0.5% per weight). The samples were irradiated for 18 hours, temperature and hardness profile were measured and the change of the surface structure was recorded.

All experiments were performed in the same way: a cylindrical container consisting of two Perspex halves fixed on a cooled base plate inside an environmental chamber was filled with the sample material. The sample with an initial height h_0 was cooled down to -100°C, while the chamber was de-pressurised. After the temperature gradient inside the sample had stabilised, the samples were irradiated using a solar simulator with an AM0 filter and the temperature profile inside the sample was measured. Additionally, a time lapse record of the morphology of the sample during the irradiation phase was obtained using a set of commercial off-the-shelf webcams.

2.1 Hardness measurements

To measure the hardness, the sample was cut in halves. The hardness profile along the vertical axis was measured using the method described by [3].
After the samples were cooled in a depressurized surrounding and irradiated each of the samples got significantly harder with a soft layer including the surface, a harder layer beneath and a softer one closer to the bottom of the sample. For samples with up to 0.2%−0.3% carbon the hardness of a subsurface layer at 3–6 cm depth increases. Samples with a higher carbon content than 0.3% show less increase in mechanical hardness.

2.2 Surface structure

The irradiation process has changed the surface significantly. During de-pressurisation a thin, homogeneous layer of carbon black accumulates on top of the sample, at that time the surface is darker than the original material. Figure 1 shows the sample surface at the beginning of the irradiation phase (left) and after 18 hours of irradiation (right).

Figure 1: Change of the surface structure after 18 hours of irradiation. Sample includes 0.5% carbon black. T_0=173K, h_0 = 15cm.

Significant changes of the sample surface can already be observed within the first few minutes of the irradiation phase. Carbon particles are emitted immediately after irradiation has started. Within the first minute this affects only small particles.
For the following few minutes, the sample surface brightens as patches of carbon particles are lifted. After some time (10 to 40 minutes, depending on the amount of carbon added) agglomerates can be seen to accrete. The more carbon black is added, the sooner the sample surface reaches maximum brightness.

Our experiments also produced large, low-density dust aggregates composed of pure carbon particles. These aggregates can reach heights of up to 5 mm if carbon content is as high as 0.5%.

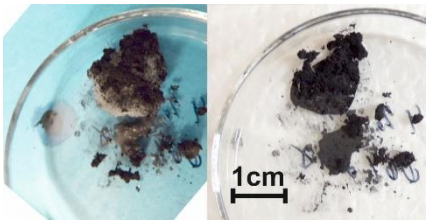

Figure 2: Images from agglomerates built up during an experiment with a 0.4% sample. Left: image taken after the agglomerate was taken of the surface. Right: same agglomerate after drying.

Samples of those surface agglomerates were collected after some of the experiments. Their structure showed remarkable mechanical strength: the carbon particles still stuck together and the agglomerates kept their shape when taken of the surface and allowed to dry (see Figure 2).

3. Summary and Conclusions

All samples were hardened considerably by exposure to solar light.
The samples reach a maximum hardness if the carbon content is 0.2% to 0.3%. No explicit hard layer can be identified if the carbon amount is higher or equal 0.4%.
The hardest layer can be found 3 - 7cm below the surface where the sample temperature is ~ 204K ±1.8K.
Particle emission starts immediately after the sample is exposed to insolation and conglomerates of carbon black built on the surface. The sample surface stays active until irradiation stops.
The evolution of the sample critically depends on where the solar energy is absorbed: at or below the surface.
We were able to produce a low-albedo dust mantle with active surface regions from an ice-dust mixture with an extremely low proportion of dust within a short period of time. This suggests caution when quantifying the bulk ratio of ice to refractory components of a real comet nucleus from remote observations alone.
The dramatic surface hardening by insolation combined with the drastic change in surface structure (even if only a marginal amount of carbon particles are added to the ice sample) suggests that cometary models should treat the nucleus surface as an interactive transitional zone to better represent cometary processes.

Acknowledgements

This project is funded by STFC under grant number ST/L000776/1.

References

[1] Kossacki, K. et al.: Comet 67P/Churyumov-Gerasimenko: hardening of the sub-surface layer**,** Icarus, Vol. 260, pp. 464-474, 2015.

[2] Sears D. W. G. et al., Laboratory simulation of the physical processes occurring on and near the surface of comet nuclei, Meteoritics & Planet. Sci., 34, 1999.

[3] Poirier, L., Lozowski, E.P and Thompson, R.I.: Ice hardness in winter sports, Cold Reg. Sci. Technol., Vol. 67, pp. 129-134, 2011.

EPSC Abstracts
Vol. 12, EPSC2018-418, 2018
European Planetary Science Congress 2018

Petrography and mineral chemistry of the ordinary chondrite NWA 11743: the first meteorite classified in a Greek-based laboratory

Avgoustos Pantazidis (1), Ioannis Baziotis (1), Ludovic Ferrière (2)
(1) Laboratory of Mineralogy and Geology, Department of Natural Resources Management and Agricultural Engineering, Agricultural University of Athens, Athens, Greece, (2) Natural History Museum, Vienna, Austria (e-mail: ibaziotis@aua.gr)

Abstract

We report here on the first meteorite – named NWA 11743 – classified in a Greek-based laboratory. We have observed both porphyritic and non-porphyritic (barred pyroxene; BP) chondrules of type-I. The meteorite matrix, commonly brecciated, is predominantly composed of olivine, low Ca-pyroxene, clinopyroxene, plagioclase, and apatite. The olivine composition ($Fa_{18.6-19.2}$) is typical for H chondrites. The BP-rich chondrules are composed of alternating bars of low- and high-Ca pyroxene. Our detailed petrographic and mineral chemistry investigations suggest that it is an H4 ordinary chondrite with a weathering stage W2.

1. Introduction

We report here on the first petrographic and mineral chemistry results obtained on the ordinary chondrite NWA 11743. The meteorite name was approved by The Meteoritical Society on March 10th, 2018. Standard methods were used to characterize the mineral end-members of the chondrules and matrix of the studied meteorite. We also call attention to the fact that this meteorite represents the first classified meteorite in a laboratory based in Greece.

1.1 Material & Methods

A small meteorite fragment of about 5.0 grams was purchased by I. Baziotis from a dealer in Marrakech, Morocco (in May 2014). The stone is a broken fragment partly covered with fusion crust. A polished thin section was prepared from the fragment and subsequently examined using optical reflected light microscopy to identify the texture and mineralogy.

Major element chemistry and textural characteristics of the matrix, mesostasis, and chondrules were obtained using a JEOL JXA-8900 Superprobe electron probe micro-analyzer at the laboratory of Mineralogy and Geology, Agricultural University of Athens (AUA), Greece. Natural mineral standards were used: quartz (Si), forsterite (Mg), corundum (Al), diopside (Ca), ilmenite (Ti, Mn), K-feldspar (K), albite (Na), fayalite (Fe), and apatite (P), at 15 kV, 15 nA, 20 s on peak counting time and 10 s for each background, and a beam diameter of 3-5 μm.

2. Petrography

Textural observations of the studied thin section in reflected light showed that it is chondritic. Petrographically, partial chondrules are quite common as well as whole chondrules (Fig. 1). The chondrules are both porphyritic and non-porphyritic, and belong to the Type-I [$Mg/(Mg+Fe^{2+})<90$]. The porphyritic olivine (PO) chondrules, rounded to oval in shape, range in size from 300-350 μm to 1200 μm.

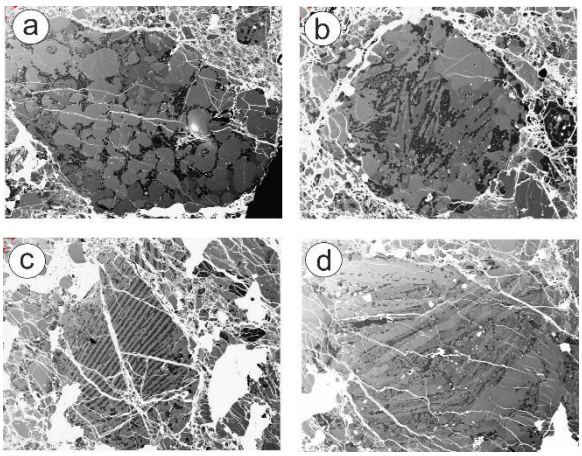

Figure 1: Backscattered electron images of the chondrules and matrix features observed in NWA 11743.

The groundmass consists of olivine (30 vol.%), low Ca-pyroxene (20 vol.%), clinopyroxene (5 vol.%), plagioclase (5 vol.%), and rare phosphate minerals (apatite). In addition, open fractures are filled with

iron oxides (40 vol.%). No shock veins were observed. The rock matrix is commonly brecciated. Black to brown fusion crust partly covers the exterior surface of the sample. Red-brown oxidation is visible on the exterior surface, around metal grains on cut surfaces, and within the matrix.

3. Mineral chemistry

The composition of olivine grains in NWA 11743 is similar to olivine from H chondrites (Fig. 1). NWA 11743 meteorite represents a coarse-grained rock with euhedral to subhedral olivine ($Fa_{18.6\text{-}19.2}$), embedded in a translucent feldspathic ($Ab_{87.6\text{-}82.8}$) glass-rich mesostasis.

The non-porphyritic chondrules are mostly of BP type, showing parallel alternating bars composed of low-Ca pyroxene ($En_{81\text{-}83}Fs_{17\text{-}18}Wo_{1\text{-}2}$) and rare high-Ca pyroxene ($En_{47}Fs_{11}Wo_{42}$) grains.

4. Classification scheme

The NWA 11743 meteorite is classified as an H4 ordinary chondrite. As shown on Fig. 2 it plots in the field of composition typical of H ordinary chondrites.

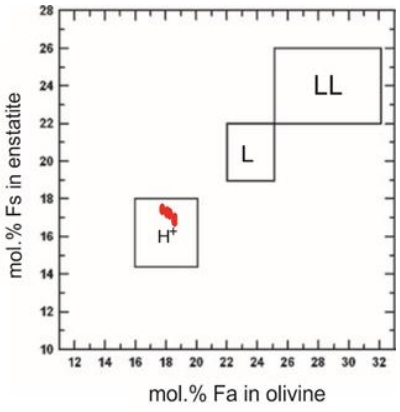

Figure 2: Plot of the chemical composition of olivine and pyroxene grains in NWA 11743. Modified from Brearley and Jones [1].

Here is a summary of the key points allowing its classification (based on [1-3]): a) The meteorite matrix is absent (type 3.2-4), and recrystallized 100% (type 4), b) Olivines with fayalite (Fa) content ranging from 18.6 to 19.2 (type 3.8-4), c). Pyroxenes are low in Ca, with mixed structure (type 4), whereas the ferrosilite (Fs) component displays a narrow range from 17 to 18 (type 4), d) Ca-phosphates (apatite) are present (type 4-6). The weathering stage is minor to slightly moderate oxidized, thus, the rocks was classified at stage W2, with the major silicate minerals being unaffected.

5. Summary and Conclusions

NWA 11743 represents an H4 ordinary chondrite. To our knowledge, it is the first meteorite to be classified in a laboratory based in Greece. The Greek government have announced earlier this year the creation of the Greek Space Agency, and our laboratory at the AUA is in process to establish the first Greek research community in planetary science research. Our main objective is to develop meteoritic science in Greece and to further contribute to the field of planetary research in Europe.

References

[1] Brearley A. J. & Jones R. H. (1998). Chondritic meteorites. In Reviews in Mineralogy, Vol. 36: Planetary Materials (Papike J. J. ed.), pp. 3-1 to 3-398. Mineralogical Society of America, Washington.

[2] Huss G. R., Rubin A. E., & Grossman J. N. (2006). Thermal metamorphism in chondrites. Meteorites and the early solar system II, 943, 567-586.

[3] Wlotzka F. (1993). A weathering scale for the ordinary chondrites. Meteoritics, 28:460.

EPSC Abstracts
Vol. 12, EPSC2018-431-1, 2018
European Planetary Science Congress 2018

Volatiles in merrillite from martian meteorite Tissint

Ioannis Baziotis[1], Mahesh Anand[2], Xuchao Zhao[2] and Ian Franchi[2]

[1]Laboratory of Mineralogy and Geology, Department of Natural Resources Management and Agricultural Engineering, Agricultural University of Athens, Athens, Greece (email: ibaziotis@aua.gr)

[2]School of Physical Sciences, The Open University, Milton Keynes, MK7 6AA, UK (email: mahesh.anand@open.ac.uk; xuchao.zhao@open.ac.uk; ian.franchi@open.ac.uk)

Abstract

We report new Cl and H isotopic data from Tissint – a martian meteorite of olivine-phyric shergottite type. Our data indicate that merrillite may accommodate up to 32 ppm of Cl, potentially representing the upper limit of Cl that can be accommodated in this nominally Cl-free phosphate. The δD values range from 721 ± 35 ‰ to 3496 ± 31 ‰, while the H_2O content is relatively modest (962 to 2341 ppm); the latter is much lower than previously reported values (all >5000 ppm), possibly representing either contamination from terrestrial environment or during sample preparation [1]. The measured δD range is possibly related to interaction of Tissint with surficial reservoirs on Mars (interaction with crustal fluids or the martian atmosphere) and/or influence of magmatic degassing.

1. Introduction

We report new Cl and H isotopic data from the martian meteorite Tissint; a well characterized depleted olivine-phyric shergottite which has been studied for its mineral chemistry, geochemistry, and shock metamorphism [2,3,4,5]. Recently, much attention has been paid to the isotopic studies and in particular that of Cl and H in merrillite from Tissint [1,6]. The overall goal of this study was to analyse the Tissint`s merrillites, which typically form at the very late stage of magma crystallization, and represent the major host of volatiles, which may provide important clues about the history of volatiles and other associated processes operating in Martian environment.

1.1 Material-Analytical Methods

Three polished thin sections were carefully examined using optical reflected light microscopy for the overall texture and mineralogy.

X-ray mapping, measurement of mineral composition and detailed textural characterization of phosphates were performed for the three polished thin sections using a JEOL JXA-8900 Superprobe electron probe micro-analyzer at the laboratory of Mineralogy and Geology, Agricultural University of Athens. Mineral standards used were: quartz (Si), forsterite (Mg), corundum (Al), diopside (Ca), ilmenite (Ti, Mn), K-feldspar (K), albite (Na), fayalite (Fe), apatite (P), at 15 kV, 15 nA, 20 sec on peak counting time, 10 sec for each background, and a beam diameter 3-5 μm. For the element maps employed to locate phosphates we used the following conditions: 15 kV, 50 nA, 100 dwell time, 2-8 μm step size and ~1μm focused beam. The merrillite isotopic analyses and the determination of the water content was performed using a Cameca NanoSIMS 50L at the Open University, UK.

2. Nano-SIMS protocol

For the NanoSIMS analyses we followed the protocol which is extensively described in [7,8], with the following modifications:

- Once in the airlock, the first sample that was analysed for Cl was left to degas under vacuum at ~55 °C for 3-4 hours, while the second one (which has been analysed for H too) for 6 hours before transferring it to the vessel chamber.
- For analysis, the beam current was 90 pA for the Cl analyses, while 600 pA was used for H.
- For Cl analysis, the raster area was 7 μm × 7 μm. For H analyses the raster area was 10 μm × 10 μm with 25% electronic gating set in order to collect only secondary ions emitted from the central zone (5 μm × 5 μm) of the analysis area.

- Secondary ion images of $^{1}H^{16}O$ (in case of Cl), and ^{1}H and ^{13}C (in case of H) were monitored in real time during pre-sputtering to ensure that the area to be analyzed was free of cracks or hotspots indicative of contamination.

- Each analysis consisted of ~10 mins cycles for Cl and ~20 mins cycles for H, corresponding to a total analysis time of about 9 min and 18 min, respectively.

3. Results

The Cl isotopic composition and Cl content were obtained from 10 merrillite grains (17 analyses). The reported $\delta^{37}Cl$ is expressed as $\delta^{37}Cl = [(^{37}Cl/^{35}Cl)_{sample}/(^{37}Cl/^{35}Cl)_{standard} - 1]*1000$, relative to Standard Mean Ocean Chloride with a defined value of 0.0 ‰. The measured $\delta^{37}Cl$ ranges from -10.7 to 7.3 ‰, although subject to large uncertainties (3.4 to 6.6 ‰) as a result of the poor counting statistics because of the very low Cl content, while the Cl content ranged from 5 to 32 ppm.

The hydrogen isotopic composition (expressed as δD) and the H_2O content have been obtained from 4 merrillite grains (5 analyses overall) that were previously analysed for their Cl isotopic ratios and content. The analysed areas suggest a large variation in δD from 721 ± 35 ‰ up to 3496 ± 31 ‰, while the H_2O content ranged from 962 to 2341 ppm; these ratios display negative correlation to each other.

4. Conclusions

Our preliminary data indicate that Tissint`s merrillite may accommodates up to 32 ppm of chlorine, potentially representing the upper limit of Cl that can be accommodated in this nominally Cl-free phosphate. Furthermore, the low H_2O content [6] confirms minimal or no contamination from terrestrial environment or during samples preparation. The δD range may associated with variable level of modification which in turn is possibly related to interaction of Tissint with surficial processes on Mars (interaction with crustal fluids or the martian atmosphere) or influence of magmatic degassing. However, additional data for H content and isotopes are needed to further evaluate the most possible scenario that gave rise to the measured volatile signatures of Tissint.

Acknowledgements

Europlanet 2020 RI has received funding from the European Union's Horizon 2020 research and innovation programme under grant agreement No 654208. We are grateful to late Prof. Lawrence A. Taylor from the University of Tennessee, USA for lending us the Tissint sections.

References

[1] Mane, P., Hervig, R., Wadhwa, M., Garvie, L. A. J., Balta, J. B., & McSween, H. Y. (2016). Hydrogen isotopic composition of the Martian mantle inferred from the newest Martian meteorite fall, Tissint. Meteoritics & Planetary Science, 51(11), 2073-2091.

[2] Aoudjehane, H. C., Avice, G., Barrat, J. A., Boudouma, O., Chen, G., Duke, M. J. M., ... & Herd, C. D. K. (2012). Tissint martian meteorite: A fresh look at the interior, surface, and atmosphere of Mars. Science, 1224514.

[3] Baziotis, I. P., Liu, Y., DeCarli, P. S., Melosh, H. J., McSween, H. Y., Bodnar, R. J., & Taylor, L. A. (2013). The Tissint Martian meteorite as evidence for the largest impact excavation. Nature Communications, 4, 1404.

[4] Liu, Y., Baziotis, I. P., Asimow, P. D., Bodnar, R. J., & Taylor, L. A. (2016). Mineral chemistry of the Tissint meteorite: Indications of two-stage crystallization in a closed system. Meteoritics & Planetary Science, 51(12), 2293-2315.

[5] Castle, N., & Herd, C. D. (2018). Experimental investigation into the effects of oxidation during petrogenesis of the Tissint meteorite. Meteoritics & Planetary Science.

[6] Bellucci, J. J., Whitehouse, M. J., John, T., Nemchin, A. A., Snape, J. F., Bland, P. A., & Benedix, G. K. (2017). Halogen and Cl isotopic systematics in Martian phosphates: Implications for the Cl cycle and surface halogen reservoirs on Mars. Earth and Planetary Science Letters, 458, 192-202.

[7] Barnes, J. J., Tartese, R., Anand, M., Mccubbin, F. M., Neal, C. R., & Franchi, I. A. (2016). Early degassing of lunar urKREEP by crust-breaching impact (s). Earth and Planetary Science Letters, 447, 84-94.

[8] Tartèse, R., Anand, M., Barnes, J. J., Starkey, N. A., Franchi, I. A., & Sano, Y. (2013). The abundance, distribution, and isotopic composition of hydrogen in the Moon as revealed by basaltic lunar samples: Implications for the volatile inventory of the Moon. Geochimica et Cosmochimica Acta, 122, 58-74.

EPSC Abstracts
Vol. 12, EPSC2018-456, 2018
European Planetary Science Congress 2018

VIS-IR spectroscopy of Alais CI chondrite by using the SPectral IMager (SPIM).

P. Manzari, S. De Angelis, M.C. De Sanctis, Istituto di Astrofisica e Planetologia Spaziali, INAF-IAPS, via Fosso del Cavaliere, 100 – 00133, Roma, (paola.manzari@iaps.inaf.it)

Abstract

In the last years increasing attention on the composition of asteroids is being payed. In fact, aside the scientific missions (Dawn for Vesta and Ceres, Osiris Rex for Bennu) other projects aim to study NEA (Near Earth Asteroids) compositional properties for monitoring, warning and defence purposes. The study of the spectral properties of the CC chondrites is important to provide new data for the interpretation of remote sensed data from class B, C and G types asteroids. The Alais meteorite is a CI chondrite that is believed to have C-G type asteroid as parent body. In this abstract we show preliminary interpretation of data collected by the Spectral Imager (SPIM) in the VIS-IR (0.45-5μm) range on powders of the Alais meteorite.

1. Introduction

The Alais meteorite is a CI chondrite that is believed to have C-G type asteroid as parent body. In this abstract we show preliminary results related to the spectral features of Alais, in the VIS-IR to support observations on C-type asteroids. Data were collected by means of SPIM SPectral Imager in the range from 0.45 to 5 μm to analyze the spectral contribution of different components of this meteorite sample thanks to the high spatial resolution (40 micrometers).
From the mineralogical point of view the Alais chondrite consists largely of a phyllosilicates matrix, mainly saponite with subordinate serpentine [1]. The composition of phyllosilicates in Alais ranges between serpentine and smectite [2]. Other phases such as carbonates, Ca-sulfate, and Mg-sulfate (epsomite and hexahydrite), do occur in veins [3,4]. Thermomagnetic analysis indicates that magnetite content is 8.9 ± 0.9 wt.%, [5]. Bulk C content is about 5.40 wt.% [6]. Recently the Alais meteorite was studied in the VNIR range by [7].

2. Experiment set up

The imaging spectrometer installed in SPIM is a spare of the spectrometer on Dawn spacecraft. It works in the 0.22-5.05 μm spectral range, with a spatial resolution of 38x38 μm on the target [8]. The analyzed samples were in the form of powders. The analyses of the absorptions were carried out on the mean spectrum of the powder and then on each pixel spectrum.

3. Results

The average spectrum of the powder is shown in fig.1. It is characterized by a blue slope in the NIR range, 1.04-2.4 μm.
It is featured by an absorption centered at 0.5 μm and around 1.16 μm. At 1.97 μm the H_2O band appears. Moving towards the IR range another weak absorption around 2.2 μm appears. The IR range show a deep absorption at 2.88 μm related to O-H stretching. Two little absorptions appear located at 3.39 and 3.49 μm that could be related to carbonates and/or to C-H contamination. The absorption near 4.26 is due to atmospheric CO_2.
The band at 4.75 μm is currently under investigation.

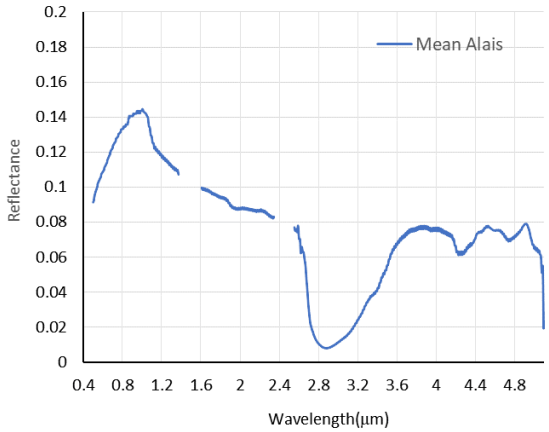

Fig. 1 Mean spectrum of powders of Alais chondrite.

Preliminary results of the analyses pixel by pixel are shown in fig.2.

The 0.49 and 1.16 μm absorptions in almost all the spectra can be assigned to magnetite: the first due to spin-forbidden Fe^{3+} absorption band transitions and the second to crystal field in octahedrally coordinated Fe^{2+}[7]. In some spectra (coordinates of pixel: x249y9; x189y9) the 1.94 μm feature appears. It is related to H_2O in hydrated phases like some sulfates and phyllosilicates. The absorptions at 2.18-2.20 μm is related to the metal-OH stretching in the phyllosilicates.

In the range between 2.7-5 μm, the spectra show higher variability in the absorption features. They are overall characterized by strong H_2O features 2.7-3 μm. Moreover, they display typical absorptions and spectral profiles of sulfates, carbonates, phyllosilicates.

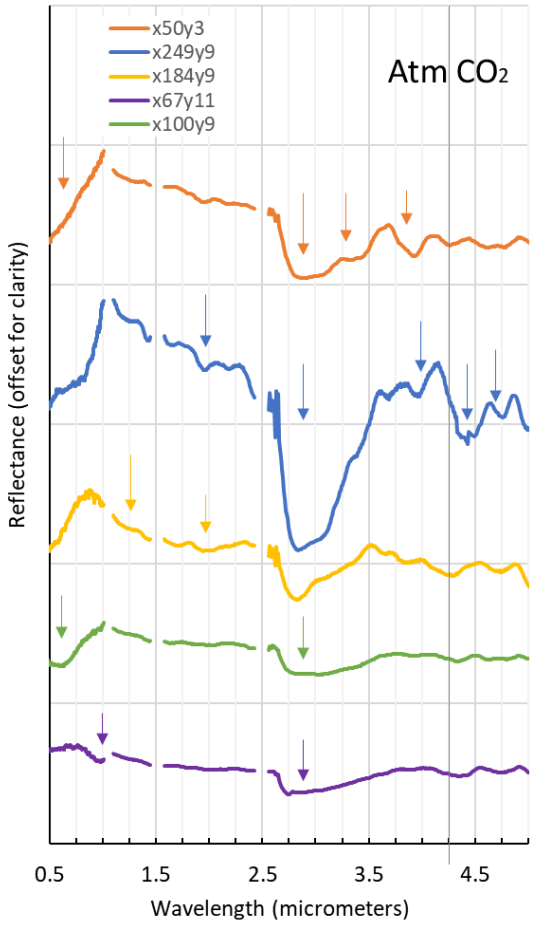

Fig. 2 Spectra of some single pixels of the Alais powder. x,y represent the coordinates of each considered pixel

For example, the spectrum related to pixel x50y3 is featured by a 3.27-3.43 μm doublet and 3.79-3.95 μm absorptions, (data around 1.5 and 2.5 μm were removed because of instrumental artifacts).

After the continuum removal these bands closest match to Mg-carbonates than Ca carbonates.

4. Summary and Conclusions

In this abstract we show some spectral properties in the VIS-IR range of powder of Alais carbonaceous chondrite. The average spectrum shows features that can be ascribed to different mineralogical groups. This first observation was confirmed by analyses of single pixels that shows the persistent occurrence of Fe-bearing minerals in the range 0.45-1.2. All the spectra investigated however show a subpixel mixing of absorptions attributable to phyllosilicates, carbonates, sulphates. Further investigations are on course with the aim to unmix the mean spectrum, quantifying each spectral phase and evaluating implications on the spectral properties of carbonaceous chondrites parent bodies.

Acknowledgements

The facility and experiment were funded by Italian Space Agency.

References

[1] Golden, D.C., Ming, D.W., Zolensky, M.E., Yang, S.V., 1994. Application of an alkylammonium method for characterization of phyllosilicates in CI chondrites. Lunar Planet. Sci. 25, 435–436 (abstract).

[2] Tomeoka, K., 1990. Matrix compositions and mineralogy of Alais and Ivuna CI carbonaceous chondrites. Lunar Planet. Sci. 21, 1256–1257 (abstract).

[3] Richardson, S.M., 1978. Vein formation in the C1 carbonaceous chondrites. Meteoritics 13, 141–159.

[4] Fredericksson, K., Kerridge, J.F., 1988. Carbonates and sulfates in CI chondrites: Formation by aqueous activity on the parent body. Meteoritics 23, 35–44.

[5] Hyman, M., Rowe, M.W., 1983. Magnetite in CI chondrites. Proc. Lunar Sci. Conf. 13, Part 2, J. Geophys. Res. 88 (Suppl.), A736–A740.

[6] Pearson, V.K., Sephton, M.A., Franchi, I.A., Gibson, J.M., Gilmour, I.A., 2006. Carbon and nitrogen in carbonaceous chondrites: Elemental abundances and stable isotope compositions. Meteorit. Planet. Sci. 41, 1899–1918.

[7] Cloutis E.A., Hiroi T., Gaffey M.J., Alexander C.M.O'D., Mann P., , 2011 Spectral reflectance properties of carbonaceous chondrites: 1. CI chondrites, Icarus, Volume 212, Issue 1.

[8] De Angelis S. Ammannito E.· Di Iorio T. · De Sanctis M.C. · Manzari P. · Liberati F.· Tarchi F. · Dami M. · Olivieri M. · Pompei C.· Mugnuolo R. (2015) The Spectral Imaging Facility: Setup Characterization, Rev. Sci. Instrum., 86.

EPSC Abstracts
Vol. 12, EPSC2018-536, 2018
European Planetary Science Congress 2018

Simulation chamber for the characterization of the bi-directional reflectance of cold planetary surfaces environments.

Y.M. Rosas Ortiz (1, 2), J. Helbert (1), A. Maturilli (1), M. Lehmann (2),
(1) Institute of Planetary Research, German Aerospace Center DLR, Berlin, Germany, (2) Technische Universität Berlin, Department of Aeronautics and Astronautics, Berlin, Germany (Y.RosasOrtiz@campus.tu-berlin.de, Joern.Helbert@dlr.de)

Abstract

In order to carryout surface experiments for planetary researches such as small bodies, cometary and Asteroidal, it is essential to reach high vacuum and cryogenic temperature. The Planetary Spectroscopy Laboratories (PSL) at the German Aerospace Center (DLR) will expand its capabilities to a low temperature range with the simulation chamber described here.

1. Research question

What are the spectral signatures of water ice that might affect the remotely detected spectral features on the icy Solar System surfaces?

1.1 Temperature Range

The Visible, IR, and Thermal Imaging Spectrometer (VIRTIS) on Rosetta obtained hyperspectral images, spectral reflectance maps, and temperature maps of the asteroid 21 Lutetia. No absorption features, of either silicates or hydrated minerals, have been detected across the observed area in the spectral range from 0.4 to 3.5 µm. The surface temperature reaches a maximum value of 245 Kelvin while the minimum retrievable temperature is 170 K [1].

1.2 Optical Range

Beck et al., 2015 [2] analyze a low-temperature reflectance spectra dependence of brucite. A strong evolution in the optical properties between 0.50 and 4.00 µm is discussed. This study discusses the likehood of brucite and the feature at 3.06 µm observed on Ceres.

Chabrillat et al., 2013 [3] present soil applications of reflectance spectroscopy, illustrating state-of-the-art methods in quantitative soil spectroscopy. The spectral range that shows good potential for retrieving information on soil attributes was discussed. The Near infrared (Near-IR) region from 1 to 5 µm contains primarily information on overtones and combinations for phylloslicates, most sorosilicates, hydroxides, some sulfates, amphiboles, carbonates, soil water and organic matter; the thermal-IR region from 5 to 100 µm contains mostly information on Si-O lattice vibrations for silicates (quartz, feldspars, clay) other than mafic, carbonate mineral group and organic compounds. To fully understand the mineralogical composition of SSSB and the implications to solar system formation and nature of water in the universe, it is necessary to investigate the whole spectral range from 1 to 100 µm, as previously proposed by Maturilli et al., 2016. [4]

2. Laboratory set-up

The simulation chamber is composed by the two external chambers, the redesigned bi-directional reflectance unit, the cryogenic sample cooling system and the vacuum pump.

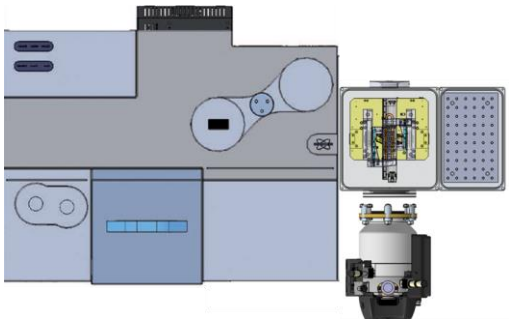

Figure 1: Top view, two external chambers attached.

3. Cooling samples

At PSL, there are currently two instruments equipped with external chambers to measure emissivity. One of them is a vacuum chamber built to measure at very high temperatures and the second chamber (that can be cooled down to 270 K) is for measurements at low to moderate temperatures. In the latter samples can be heated from room temperature to 420 K in a purging environment. The sample compartment on the spectrometer has been used to simulate the low-T chamber and a cooling sample container has been designed and adapted to the reflectance unit. The icy-samples have been cooled down to 190 K using a full controlled freezer and they have been kept cool using liquid nitrogen. Figure 2 shows the redesigned reflectance unite.

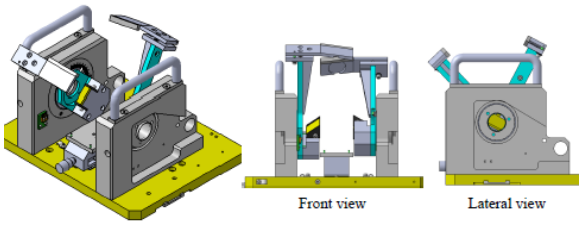

Figure 2: The redesigned reflectance unit can perform bi-directional reflectance measurements with independent incident and emission angles from 13 to 85°.

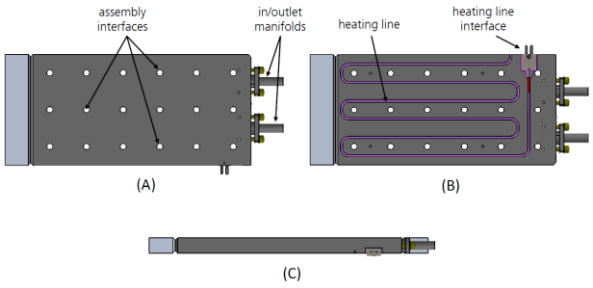

Figure 3: Concept design cooling plate. (A) Top view showing different contact points for the assembly interface with the sample plate; fitting also standard hardware. (B) Bottom view showing the thermocouple as a heating line for the temperature control system, the cooling line inlet and output manifolds are shown. (C) Left view.

A concept design is shown on Figure 3 where the cooling line is fully immersed in the material, the interface area is on the top side having only one cooling system loop, this concept is widely proof as a stable low temperature closed-cycle cryostat. Utilizing thermal conductivity material, temperature control system, and easy-to-use system. The table 1 summarizes its features.

Table 1: This is the example of an included table

Material	Copper Or Aluminum
Bolt arrange	3 x 6
Dimensions	55 x 120 mm^2
Thickness	5 mm
Cooling loop system	Liquid Cooled, LN2
Cooling line	2 lines, LN2 Immersed
Temp. range	100 - 350 K
Temp. stability	1 K or less
Control connections	1 heater, LN2 in/outlet
Orientation	Any position
Cooldown Consumption	0.4 liters LN2
Operational Consumption	0.6 L/hr at 5 K w/LN2

Summary and Conclusions

In summary, laboratory spectroscopy investigations of minerals are key to support the interpretation of remote sensing data returned by the interplanetary missions. A simulation chamber for FT-spectroscopy experiments at the PSL is currently under development. The expected cryogenic temperature to reach is approximately within the range of 70K – 100K. The potential experiments are promising. The current and future missions (e.g., NASA/DAWN and ESA/ExoMars 2020, NASA/EUROPA Multiple Flyby Mission, ESA/JUICE respectively) indicate the high potential usage of this development, which may result in many scientific or even commercial applications.

References

[1] Coradini, A. et al. (2011). "The surface composition and temperature of Asteroid 21 Lutetia as observed by Rosetta/VIRTIS". In: Science 334.6055, 492–494. doi: 10.1126/science. 1204062

[2] Beck, P., at al. (2015) Low-temperature reflectance spectra of brucite and the primitive surface of 1-Ceres?, Icarus 257. doi: 10.1016/j. icarus.2015. 05.031

[3] Chabrillat, S. et al. (2013). "Quantitative Soil Spectroscopy". In: Applied and Environmental Soil Science 2013.616578, p. 3. doi: 10.1155/2013/616578

[4] Maturilli, A. et al. (2016) Characterization of asteroid analogues by means of emission and reflectance spectroscopy in the 1 to 100µm spectral range, Earth, Planets and Space. doi: 10.1186/s40623-016-0489-y

EPSC Abstracts
Vol. 12, EPSC2018-672, 2018
European Planetary Science Congress 2018

INVESTIGATING REFLECTANCE PROPERTIES OF SPACE WEATHERED SILICATES: EFFECT OF SWIFT HEAVY ION IRRADIATION

Cristian Carli (1), Rosario Brunetto (2), Giovanni Strazzulla (3), Giovanna Serventi (4), Francois Poulet (2), Fabrizio Capaccioni (1), Yves Langevin (2), Emmanuel Gardes (5), Rafael Martinez R. (5), Philippe Boduch (5), Alicja Domaracka (5), and Hermann Rothard (5)
(1) IAPS-INAF (Roma, Italy; cristian.carli@iaps.inaf.it), (2) IAS-CNRS (Orsay, France), (3) OACT-INAF (Catania, Italy) , (4) University of Parma (Parma, Italy), (5) CIMAP-Ganil, Normandie Univ, ENSICAEN, UNICAEN, CEA, CNRS (Caen, France)

Abstract

Space weathering strongly interests the surface of Mercury, affecting the characteristics of minerals and rocks. Here, we investigate the spectral variability from visible to mid infrared on three different silicates, partially covered by a thin film of carbon, irradiated with swift heavy ion at three increasing fluences. Ions and carbon affect spectral properties in different way from visible to near infrared (VNIR); whereas in mid infrared (MIR) only irradiation seems to contribute, describing an increasing process of silicate's amorphization.

1. Introduction

Mercury's surface can be strongly affected by weathering processes, due to the proximity of the Sun and the absence of atmosphere. Space weathering interests in different way the material present on the surface, inducing deformation and vacancy on the crystal lattice. Thus, spectral properties, from the VNIR to the MIR, can be affected by the environment (e.g. [1]).

MESSENGER mission results highlighted that Mercury's surface is mainly volcanic in origin, spectrally variegate, with evidences indicating low FeO in silicates (e.g. <1% [2]). The surface elementary composition has been analyzed by XRS and GRS [3], results suggest the presence of different geochemical terrains with composition that varies from high Mg/Si, in older plains with high Ca/Si, locally high S/Si, and low Al/Si ratios. Northern young plains have higher Al/Si, Na, K, and lower Mg/Si, Ca/Si [e.g. 4]. C was suggested as rest of a primary crust due to floating of graphite [5,6]. Thus, olivine (ol), pyroxene, plagioclase (pl), quartz, and in minor abundance, corundum, nepheline (neph), and Mg-Ca sulfides are proposed as principal minerals in the crust [e.g. 7,8].

Here, we present a spectral study of swift heavy ion irradiation of three silicates, ol, neph, and pl as a simulation of heavy ion irradiation of Mercury.

2. Samples

Four cm-sized chips were prepared for each mineral, Ol (Fo90), neph and pl (anorthitic). Half of the surface of each was covered with a thin film of carbon (C). Three chips of each mineral were irradiated at GANIL-IRRSUD (France) with 88 MeV $^{129}Xe^{23+}$ ion with fluences of 10^{11}, 10^{12} and 10^{13} ions/cm^2. The sputtering of nepheline was investigated in [9].

3. Analytical Methods

Spectra were acquired from the VNIR to the MIR (0.4-15 μm) on the unirradiated and irradiated targets. Two setups were used: a) The VNIR spectra were acquired at IAS-Orsay in a diffuse bidirectional configuration, i 30° and e 0°, using a grating spectrometer Maya2000 Pro (Ocean Optics), coupled to an optical microscope; b) The NIR-MIR confocal reflectance was investigated with FTIR micro-spectrometers (Agilent Cary 670/620, Thermo Scientific Continum XL and iN10) available at SMIS beamline of synchrotron SOLEIL.

4. Results

Preliminary analyses show that: 1) in the VNIR the film of C reduces the reflectance; 2) reflectance for samples without C increases in the NIR and it decreases in the VIS, with a consequent reddening, with increasing the ion fluence; 3) in the MIR, C has no effect, the Christiansen Feature has no evident

shift, whereas the Reststrahlen band peaks are shifted with increasing fluence. This continues until the highest fluence, where the samples show signs of amorphisation (Fig.1), and a strong reduction of the absorption area up to 40% (Fig.2). Similar trends were observed in ion irradiated meteorites [10,11].

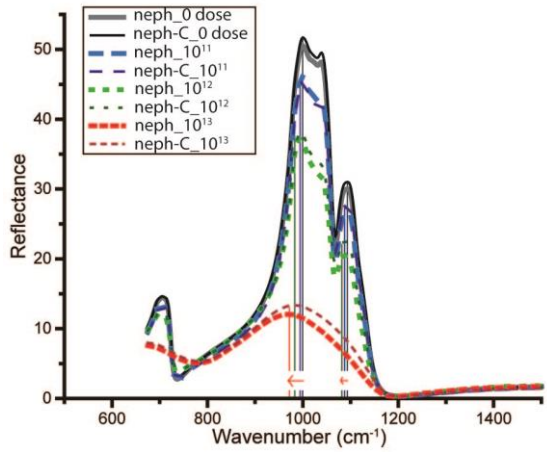

Figure 1: TIR nepheline spectra with different fluences; we highlighted the major shifts (red arrows).

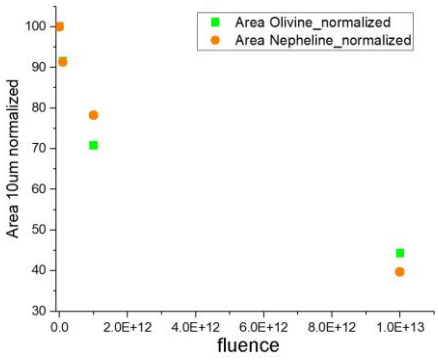

Figure 2: Normalized Reststrahlen absorption area at different fluences shows a similar intensity reduction for all silicates.

5. Future works

In preparation of BepiColombo mission, where VNIR and MIR will be investigated by SIMBIO-SYS and MERTIS [12], we plan to investigate several samples, natural and Mercury-like synthetic samples, as suggested by [6,7], and other irradiation conditions than those presented here (e.g. lighter ions and lower energies).

Acknowledgements

This research was supported by ASI, SIMBIO-SYS project. The microspectroscopy activities are supported by grants from Région Ile-de-France (DIM-ACAV) and SOLEIL. Authors thanks to F.Borondics, C.Sandt, and N.Bott for help and support at SOLEIL and A.Doressoundiram for discussion.

References

[1] Domingue D.L. et al., 2014.: Mercury's Weather-Beaten Surface: Understanding Mercury in the Context of Lunar and Asteroidal Space Weathering Studies, Sp.Sci.Rev. 181, 121–214.

[2] Klima R.. et al., Visible to near-infrared hyperspectral measurements of Mercury: challenges for deciphering surface mineralogy, Whispers, July 2014.

[3] Solomon S.C. et al., 2007.: MESSENGER Mission Overview, Sp.Sci.Rev., 131, 3-39.

[4] Weider S.Z. et al., 2015.: Evidence for geochemical terranes on Mercury: Global mapping of major elements with MESSENGER's X-Ray Spectrometer, EPSL, 416, 109–120.

[5] Peplowski P.N. et al., 2016.: Remote sensing evidence for an ancient carbon-bearing crust on Mercury, Nature Geoscience, 9, 273-276.

[6] Vander Kaaden K.E. and McCubbin F. 2015.: Exotic crust formation on Mercury: Consequences of a shallow, FeO-poor mantle, JGR 120, 195-209.

[7] Namur O. et al. 2016.: Melting processes and mantle sources of lavas on Mercury, EPSL 439, 117-128.

[8] Vander Kaaden K.E. et al. 2017.: Geochemistry, mineralogy, and petrology of boninitic and komatiitic rocks on the mercurian surface: Insights into the mercurian mantle Icarus 285, 155–168.

[9] Martinez et al. 2017.: Sputtering of sodium and potassium from nepheline: Secondary ion yields and velocity spectra, NIMPB, 406, 523-528.

[10] Brunetto R. et al. 2014.: Ion irradiation of Allende meteorite probed by visible, IR, and Raman spectroscopies, Icarus, 237, 278-292.

[11] Lantz C. et al. 2017.: Ion irradiation of carbonaceous chondrites: A new view of space weathering on primitive asteroids, Icarus, 285, 43-57

[12] Benkhoff J. et al. 2010.: BepiColombo—Comprehensive exploration of Mercury: Mission overview and science goals, PSS 58, 2-20.

EPSC Abstracts
Vol. 12, EPSC2018-674, 2018
European Planetary Science Congress 2018

Design, Development and Testing of an Environmental P-T Cell for InfraRed Spectroscopy Measurements.

S. De Angelis[1], M. Ferrari[1], M.C. De Sanctis[1], D. Biondi[1], A. Boccaccini[1], M.Formisano[1], A. Morbidini[1], E. Ammannito[1-2], T. Di Iorio[1-3].
[1]IAPS-INAF (via del Fosso del Cavaliere, 100, 00133, Rome, Italy; simone.deangelis@iaps.inaf.it), [2]ASI, Rome, Italy,
[3]ENEA SSPT-PROTER-OAC, Centro Ricerche Casaccia, Via Anguillarese 301, 00123, Roma, Italy

Introduction

Infrared spectra of minerals and rocks acquired in the laboratory are often dominated by the presence of absorption features due to adsorbed water. Frequently H_2O molecules from ambient water vapor, at standard P-T conditions, are subject to physical adsorption: the molecules quickly attach between the surface grains of the materials (especially powders, but also slabs) both during the preparation, storage and measuring phases. Fundamental absorption features due to OH-stretching and H-O-H bending transitions in water occur in the 3-6-µm spectral region, while overtones and combinations occur in the 0.9-2.5-µm region [1,2]. These absorptions can often mask diagnostic bands characteristic of the host materials, and this can also be problematic when using laboratory spectra for comparison and interpretation of data from planetary missions. In order to overcome these issues, we designed and developed an environmental cell to acquire infrared reflectance spectra of materials under controlled pressure and temperature.

1. Cell Design

The vacuum chamber was realized custom by Vacom, while other parts were realized custom at INAF-IAPS. The sample to be measured is placed in a copper sample holder, which is in contact with a ceramic heater, that allows to warm up to 400 °C. The temperature control is performed thanks to a PID controller. The cell consists of a UHV stainless steel cube: a primary diaphragm membrane pump and a secondary turbomolecular pump in the current version permit to reach a vacuum of about 10^{-5} mbar within the cell. A 3-mm thick transparent CaF_2 window allows acquiring spectra in the visible-infrared range. Both the sample holder and ceramic heater are 25.4 mm in diameter, while the viewport diameter is 40 mm. The total height of the cell is about 50 mm.

2. Preliminary tests.

We performed numerous tests with various types of powder samples, mostly phyllosilicates with different hydration states, using a FieldSpec Pro spectro-photometer in the range 0.35-2.5 µm and a QTH lamp. Test spectra were acquired in continuously-running mode by placing a sample within the cell, then pumping from ambient pressure down to $10^{-4}\div10^{-5}$ mbar, and keeping fixed the temperature at room values.
In the pumping phase the sample lost almost all the adsorbed water. We start the heating phase once that the limit pressure is reached. Further spectra were acquired at different temperatures in the range 20÷300 °C. Most of the samples lost all their water above 150-200 °C. At higher temperatures (T>240÷250 °C) we register the dehydroxylation process for a few phyllosilicates, in accordance with the TGA data for these minerals.

3. Example: Hectorite

The spectra of hectorite (SHCa_1) acquired during the initial pumping phase from 10^{3} down to 10^{-4} mbar are shown in figure 1. The water absorptions located at 1.4 and 1.9 µm almost disappear during the pumping. The absorption band near 2.3 µm, likely due to Mg-OH, remains quite unaltered. The spectra of hectorite acquired in vacuum (10^{-4} mbar) during the subsequent heating phase are shown in figure 2. The room P-T spectrum (red) is shown for comparison. Spectra have been acquired during the

temperature ramp 50-250 °C. The mineral experiences oxidation for T>240 °C, as evidenced by the decreasing of reflectance and change in spectral shape.

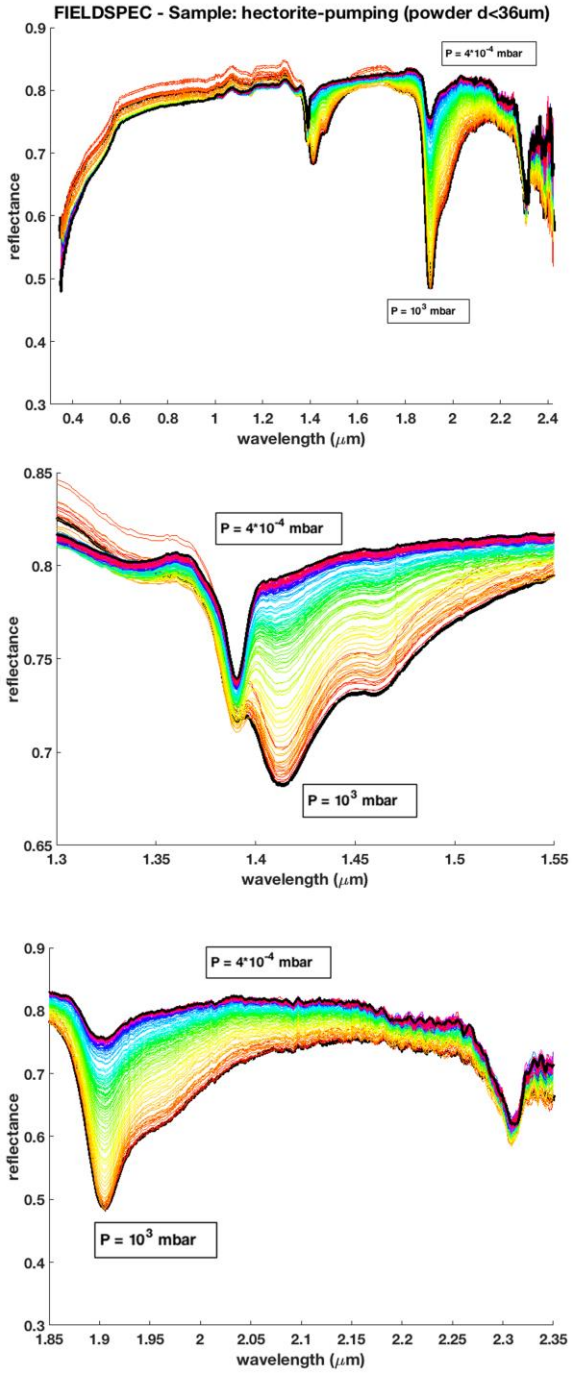

Fig. 1. Spectra of hectorite, acquired with FieldSpec Pro during the pumping phase, from 10^3 to 10^{-4} mbar. The water absorptions at 1.4 and 1.9 μm almost disappear during the pumping.

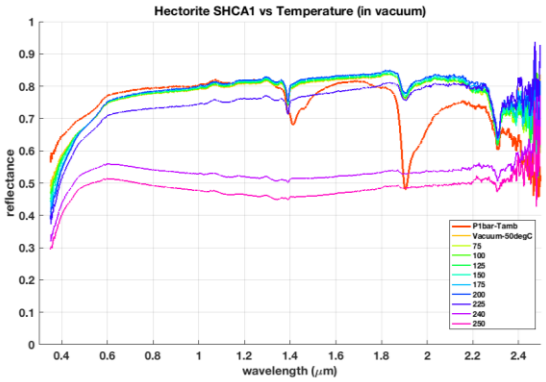

Fig. 2. Spectra of hectorite acquired with FieldSpec Pro in vacuum, during the heating phase. The starting spectrum (room P-T) is in red, for comparison. Spectra are acquired during the temperature ramp 50-250 °C.

Acknowledgements

This work is supported by the Italian Space Agency.

References

[1] Farmer, V. C.: *The vibrations of protons in minerals: hydroxyl, water, and ammonium*, in *The infrared spectra of minerals*, edited by V. C. Farmer, pp. 137-181, Mineralogical Society, London, 1974.
[2] Clark, R.N., et al: *High spectral resolution reflectance spectroscopy of minerals*. Journal of Geophysical Research 95 (B8), 12653–12680, 1990

EPSC Abstracts
Vol. 12, EPSC2018-683, 2018
European Planetary Science Congress 2018

From laser experiments to nature: How accurately can we reproduce space weathering?

Agnese Fazio (1), Dennis Harries (1), Doreen Schmidt (1), Kilian Pollok (1), and Falko Langenhorst (1,2)
(1) Analytical Mineralogy of Nano- and Microstructures, Institute of Geosciences, Friedrich Schiller University Jena, Germany (Agnese.Fazio@uni-jena.de) (2) Hawai'i Institute of Geophysics and Planetology, School of Ocean and Earth Science and Technology, University of Hawai'i at Manoa, USA.

Abstract

The present contribution aims to discuss the possibility to reproduce space weathering effects via femtosecond laser experiments in the light of space weathering defects found in Hayabusa regolith grains.

1. Introduction

The surfaces of the airless solid bodies of the solar system are exposed to the irradiation of the solar wind and to the bombardment of micrometeoroids. The ensemble of the effects caused by these surface processes is known as space weathering [1].

Since the first recognition of space weathering in nature, numerous experiments have been successfully carried out to reproduce its spectral effects. The most common experiments are ion irradiation (simulation of the solar wind; [2]) and nanosecond laser experiments (simulation of micrometeoroid impacts [2-4]). Only a few studies further investigated the microstructural modifications produced by the experiments [5, 6], probably due to the paucity of regolith materials to compare with.

Nowadays, the only regolith material available is from the surfaces of the Moon and asteroid 25143 Itokawa [7, 8]. The sample return missions are a new frontier of the space exploration and in the following years, other regolith materials will be available. These missions are the key to understand surface processes on primitive bodies in the solar system.

In this work, we present the results of an investigation of Itokawa grains. These natural observations will be compared to results femtosecond laser experiments to assess the capabilities of this experimental approach to reproduce space weathering effects [9, 10].

2. Samples and Methods

In the framework of 4th International Announcement of Opportunity for Hayabusa sample investigation, we received five Itokawa particles. Currently we have focused on the investigation of particle RB-QD04-0092, which was sliced by focused ion beam (FIB) and then studied by analytical transmission electron microscopy (TEM).

3. Observations on RB-QD04-0092

The RB-QD04-0092 is a flat grain (29 x 25 x 8 µm) consisting of enstatite (En_{75-80}) and olivine (Fo_{71-78}). The grain shows a polycrystalline rim, that indicates an exposure to the solar wind [11]. Solar flare tracks have been found in both minerals and their density is comparable with literature data (10^8 – 10^9 cm^{-2}; [12, 13]). In addition to these features, olivine and enstatite show typical shock effects known for shocked meteorites, that is, [001] dislocations in olivine and clinoenstatite lamellae. This is the first report of clinoenstatite lamellae in Hayabusa-returned samples.

Contrary to other literature observations, no (sulfur)-iron nanoparticles and amorphized rims [7] have been found. The absence of these features can be explained either due to the superimposition of the irradiation of solar wind or due to the gardening process and secondary impacts. A combination of both mechanisms is also possible.

4. Femtosecond laser experiments

Recent femtosecond laser experiments considerably improved the state-of-the-art knowledge on space weathering [9, 10]. The irradiation with femtosecond laser light induces a nanosecond shock wave with the initial pressure of several tens GPa, which results in the formation of microcraters with a layered

subsurface structure, similar to those observed in lunar samples [14]. The topmost layer is amorphous. In olivine, it can be partially recrystallized and contains iron nanoparticles in its lowermost part. The underlying layer is defect-rich. In olivine, it is dominated by dislocations [9], instead, in pyroxenes, parallel planar lamellae (amorphous in the upper part) and clinoenstatite lamellae are common [10]. Reflectance spectra of both minerals are altered, similarly to space weathered asteroid surfaces [9].

5. Conclusions

The preliminary comparison of the microstructural features of Itokawa regolith and irradiated minerals supports the employment of the femtosecond laser experiments for reproducing and characterizing the shock defect modifications. Although the spectral alteration of natural and experimental materials is similar, the mechanisms of formation of the amorphous layer and the iron nanoparticles might be different, because the experimental irradiation with laser light is not comparable with the natural bombardment with solar wind particles. To improve the understanding of these mechanisms and of the impact history of asteroidal regolith, further experimental studies and observations on Hayabusa-returned grains will be necessary.

Acknowledgements

This work is supported by the research unit FOR 2285 “Debris Disk in Planetary Systems” of the DFG (LA 830/20-1). The FIB-TEM facility at FSU Jena is supported by DFG grant LA 830/14-1. The authors are grateful to JAXA for providing Itokawa regolith grains. The Alexander von Humboldt Foundation is acknowledged for making this collaboration possible.

References

[1] Bennett C.J., Pirim C., and Orlando T.M. (2013) Space-Weathering of Solar System Bodies: A Laboratory Perspective. Chemical Reviews 113:9086-9150.

[2] Yamada M., Sasaki S., Nagahara H., et al. (1999) Simulation of space weathering of planet-forming materials: Nanosecond pulse laser irradiation and proton implantation on olivine and pyroxene samples. Earth Planets and Space 51:1255-1265.

[3] Brunetto R., Romano F., Blanco A., et al. (2006) Space weathering of silicates simulated by nanosecond pulse UV excimer laser. Icarus 180:546-554.

[4] Loeffler M.J., Baragiola R.A., and Murayama M. (2008) Laboratory simulations of redeposition of impact ejecta on mineral surfaces. Icarus 196:285-292.

[5] Sasaki S., Nakamura K., Hamabe Y., et al. (2001) Production of iron nanoparticles by laser irradiation in a simulation of lunar-like space weathering. Nature 410:555-557.

[6] Loeffler M.J., Dukes C.A., Christoffersen R., et al. (2016) Space weathering of silicates simulated by successive laser irradiation: In situ reflectance measurements of Fo(90), Fo(99+), and SiO2. Meteoritics & Planetary Science 51:261-275.

[7] Noguchi T., Nakamura T., Kimura M., et al. (2011) Incipient Space Weathering Observed on the Surface of Itokawa Dust Particles. Science 333:1121-1125.

[8] Keller L.P. and Mckay D.S. (1993) Discovery of Vapor Deposits in the Lunar Regolith. Science 261:1305-1307.

[9] Fazio A., Harries D., Matthäus G., et al. (2018) Femtosecond laser irradiation of olivine single crystals: Experimental simulation of space weathering. Icarus 299:240-252.

[10] Schmidt D., Pollok K., Matthäus G., et al. (2018) Space weathering in enstatite single crystals: Femtosecond laser pulse experiments simulate micrometeoroid impacts. European Planetary Science Congress 2018.

[11] Harries D., Matsumoto T., Fazio A., et al. (2018) Solar wind-induced space weathering on asteroid Itokawa. European Planetary Science Congress 2018

[12] Harries D. and Langenhorst F. (2014) The mineralogy and space weathering of a regolith grain from 25143 Itokawa and the possibility of annealed solar wind damage. Earth Planets and Space 66.

[13] Keller L.P. and Berger E.L. (2014) A transmission electron microscope study of Itokawa regolith grains. Earth Planets and Space 66.

[14] Noble S.K., Keller L., Christoffersen R., et al. (2016) The microstructure of lunar micrometeorite impact craters. Lunar and Planetary Science Conference.

EPSC Abstracts
Vol. 12, EPSC2018-788, 2018
European Planetary Science Congress 2018

Reflectance of low-albedo dusts and water ice mixtures. Application to the surface of comet 67P.

Z. Yoldi (1), A. Pommerol (1) and N. Thomas (1).
(1) Physikalisches Inst., University of Bern, Sidlerstrasse 5, CH-3012 Bern, Switzerland (zurine.yoldi@space.unibe.ch)

1. Introduction

Even though it is admitted that cometary nuclei are ice-rich in bulk, comets present extremely low albedo at their surface. The case of the comet 67P is not different; its water content at the surface has been estimated to be lower than 10 wt% from its reflectance spectrum [1].

Back in 2015, we measured the bidirectional visible reflectance of intimate mixtures of grained water ice and referenced lunar regolith simulant JSC1-AF [2]. We observed that it is possible to mix up to 75 wt% of ice within the dust without increasing its reflectance notably, therefore making this ice hardly detectable for visible imagers.

Here, we present the reflectance of these samples extended to the near-IR (up to 2.4 μm). We have also used a powder darker than JSC1-AF, as well as tried other association modes between dust and water ice, such as frost deposition. We propose a way to distinguish between frost and intimate mixing only from the reflectance spectra, without the need of reflectance models.

2. Samples

On the one side, we have repeated the intimate mixtures with JSC1-AF and water ice, whose preparation is fully detailed in [2]. We have prepared the same kind of mixtures with a darker basalt, described in [3].

On the other side, we have condensed frost onto the dark basalt. To do so, we have designed and built a sample holder that allows to cold trap atmospheric water on the powder. We have measured three different thicknesses of frost layers, which we estimate to be from the micrometres to hundreds of micrometres thick.

The reflectance measurements have been acquired with the Simulation Chamber for Imaging the Temporal Evolution of Analogue Samples (SCITEAS), at the Laboratory for Outflow Studies of Sublimating icy materials (LOSSy) [4].

We have performed spectral analysis by computing the depth of the water bands and the visible and near-infrared spectral slopes.

3. Results

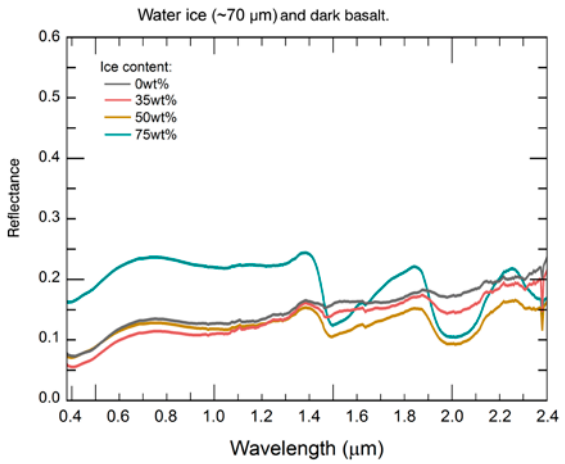

Figure 1 Reflectance spectra of various intimate mixtures of water ice and dark basalt.

Figure 1 shows the reflectance of intimate mixtures of water ice and dark basalt. As observed in [2], the reflectance in the visible range of the reflectance spectrum only rises when water ice is present in more than a 50 wt%.

Figure 2 shows the effect of frost deposition on the reflectance of dark basalt. The different curves represent the estimated thickness of the frost layers on top of the powders.

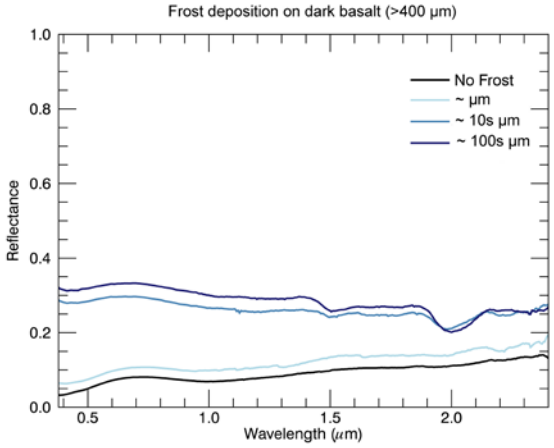

Figure 2 Various layers of water frost on a sample of dark basalt with grains bigger than 400 µm

4. Discussion

Looking at Figures 1 and 2, we understand the different effect that water has on reflectance depending on if it is present as frost or intimately mixed. Nevertheless, when we look at a cometary surface, it is not straightforward to distinguish frost from intimate mixtures.

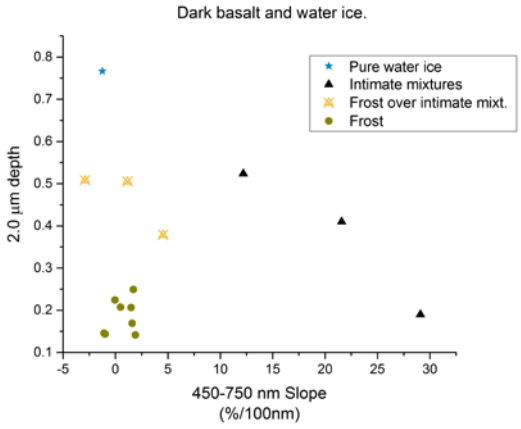

Figure 3 Comparison of the depth of the H_2O band at 2.0 µm with the VIS spectral slope for various association modes

Figure 3 shows how the comparison of spectral parameters can help to discern different association modes between soil and water ice.

In this conference, we present the application of these methods to the surface of comet 67 P.

Acknowledgements

This work has been carried out within the framework of the NCCR PlanetS supported by the Swiss National Science.

References

[1] Filacchione et al. (2016) Nature, 529, pages 368–372.
[2] Yoldi et al. (2015) GRL, *42*, 6205-6212.
[3] Pommerol et al., (2013) JGR, 118. 2045-2072.
[4] Pommerol et al., (2015a). PSS., Vol 109-110.

EPSC Abstracts
Vol. 12, EPSC2018-883, 2018
European Planetary Science Congress 2018

Raman and XRF analysis of the new NWA 11273 Lunar meteorite.

Jennifer Huidobro, Julene Aramendia and Juan Manuel Madariaga.
Department of Analytical Chemistry, University of the Basque Country UPV/EHU, P.O. Box 644, E-48080 Bilbao, Spain.
(julene.aramendia@ehu.eus)

Abstract

Until today, there are not scientific publications about the geochemical composition of the NWA 11273 Lunar meteorite, officially included in Meteoretical Bulletin Database in 2017. However, its analysis could give more data about the geo-chemical composition of the lunar surface and the conditions suffered by the meteorite until its arrival to the Earth. Considering this, Raman spectroscopy and X-Ray Fluorescence were employed in order to obtain a first map of the elemental and mineralogical composition of this meteorite. In this way, several silicates, phosphates and sulphates were detected.

1. Introduction

Apollo and Luna missions brought to Earth Moon surface samples which still are under analysis to gain knowledge [1]. The collected samples and the Lunar Meteorites are the extraterrestrial materials used to answer the questions arisen along the time about the composition, origin and evolution of the Earth natural satellite. Nowadays, despite of the fact that the composition of the mantle is still debated, the feldspar is fairly sure to be the main compound in the surface. These feldspars appear in certain areas together with the so-called mare basalts. To provide more data about the composition of the Moon, the NorthWest Africa (NWA) 11273, a recently (2017) included Lunar Meteorite in the Meteoretical Bulletin Database, has been studied in this work. Until now, there are not scientific works published about this meteorite so far. Therefore, this study will be focused on the analysis of the mentioned specimen by using non-destructive analytical techniques to ascertain the elements contained in the surface and the different mineral phases, as a first step to further accomplish the analysis inside the body of the different specimens in our hands.

2. Sample description

The NWA 11273 meteorite is a Lunar feldspathic breccia [2]. It was found buried in Algeria in 2017. It is said to be composed by clasts of anorthite, olivine, pigeonite, augite, chromite, Ti-Cr-Fe spinel, kamacite, taenite and troilite. Rare basalt clasts and glass fragments are said to be also present. However, no official peer reviewed works extend this information.

The analyzed specimen is a polished slice without crust belonging to the University of the Basque Country (collection of the IBeA research group).

3. Materials and methods

In order to obtain as much information as possible but preserving the sample for further analysis, non-destructive analytical techniques were employed as a first step of the specimen study. In this way, Raman spectroscopy, for obtaining molecular information, and X-Ray fluorescence (XRF), for elemental analysis, were selected as the most suitable techniques [3]. The Raman spectroscopy analyses were performed using a InVia confocal micro-Raman spectrometer (Renishaw, UK), provided with a 785 and 532 nm excitation lasers and a CCD detector working in both point by point and Raman image mode, using laser power filters to avoid thermal transformations, with a resolution of 1 cm^{-1}. The XRF analyses were conducted with a M4 TORNADO micro-spectrometer, in point-by-point and image modes with spatial resolution down to 25 µm, for Mo Kα radiation, that can be increased up to 200 µm.

4. Results and discussion

By means of XRF analysis it was seen that the major elements (beyond a 0.1% w/w) present in the sample were Si, Ca, Al, Fe and Mg (Figure 1). Moreover, other minor elements were also detected such as Mn, Ti, K, Ni, S, Na, Cr, Sr and Zr. Some metallic areas were also distinguished composed by Fe and Ni.

Raman spectroscopy gave us the molecular (mineralogical) composition in the different areas of the surface of NWA 11273. It has to mention that anorthite was the main detected phase together with olivine, augite and other pyroxenes, as it was expected [2]. It is worthy to point out that the olivine ranges, calculated from the two main Raman bands, are in concordance with those ranges stated in the unique information source about this meteorite [2]. In this study, the olivines ranged from Fo56-Fa44 to Fo83-Fa17 and in the mentioned source [2], went from Fo40.3-Fa59.7 to Fo91.3-Fa8.7. This is in agreement with the pink color distribution, seen in Figure 1 that corresponds to the areas where magnesium is the major element.

Apart from the expected ones, other mineral phases such as zircon and apatite were also found. The case of the zircon deserves a special mention since the Raman band appeared at 1006 cm^{-1} instead of 1008-1010 cm^{-1} where the non-shocked zircon appears. This band shift occurs when the zircon has been subjected to pressures around 20 GPa [4]. This pressure effect is also observed in the zircon band at 439 cm^{-1} which is shifted in the zircon detected in this work to 441 cm^{-1}. This finding proves that the specimen was subjected to high pressures probably when ejected from the surface of the Moon.

In addition, a sulphate with its main Raman band at 987-988 cm^{-1} was detected. This is an important discovery as no sulphates have been so far related to the Moon composition. Unfortunately, no secondary Raman bands were clearly detected in our study and therefore the exact identification of the sulphate resulted impossible. Notwithstanding, by overlapping Raman and XRF results on the area where the sulphate was detected, it was seen that the main elements were sulphur and nickel; therefore, it can be thought that the detected compound was a nickel sulphate. Actually, the main Raman band could coincide with dwornikite ($NiSO_4 \cdot H_2O$) or regertsite ($NiSO_4 \cdot 6H_2O$). However, this hypothesis must be sustained with further analyses to confirm the presence of water of crystallization.

Besides, calcite and hematite were identified in the surface of the meteorite. They are thought to appear due to weathering process. For instance, calcite is always related to veins and cracks. Regarding hematite, it could appear by the oxidation of the mentioned metallic areas as its presence is only as minor grains.

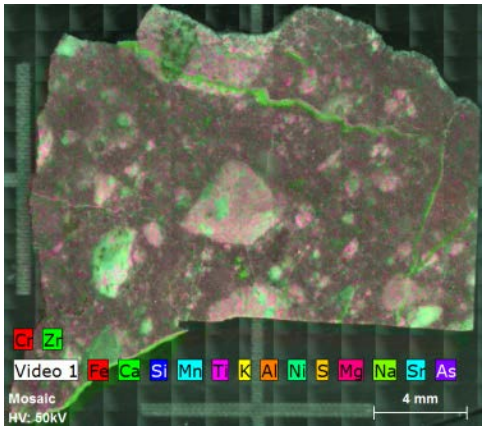

Figure 1. XRF image of the NWA 11273 meteorite showing the distribution of the major elements.

5. Conclusions

As a conclusion, it can be said, that the analysis of new meteorites could provide valuable data about the original composition and the physical-chemical processes that are taking place in our natural satellite. It is also crucial to distinguish between the weathering processes that a meteorite suffered once in the Earth with the weathering processes that the rocks suffer in the past on the Moon surface. Finally, it should be pointed out the importance of the apatite and sulphate findings, arisen from the study of the NWA11273 Lunar meteorite.

Acknowledgements

This work has been financially supported through the Exomars-Raman project (ref. ESP2017-87690-C3-1-R), funded by the Spanish Agency for Research AEI (MINEICO-FEDER/UE).

References

[1] http://lunarexploration.esa.int/#/intro

[2] https://www.lpi.usra.edu/meteor/metbull.php?code=66064

[3] Aramendia J., Gomez-Nubla L., Castro K., Fdez-Ortiz de Vallejuelo S., Arana G., Maguregui M., Baonza V.G., Medina J., Rull F., Madariaga J.M.: Overview of the techniques used for the study of non-terrestrial bodies: Proposition of novel non-destructive methodology, TrAC, Vol. 98, pp. 36-46, 2018.

[4] Gucsik A., Zhang M., Koeberl C., Salje E. K. H., T. Redfern S. A., Pruneda J. M.: Infrared and Raman spectra of ZrSiO4 experimentally shocked at high pressures, Mineralogical Magazine, Vol. 68, pp. 801-811, 2004.

EPSC Abstracts
Vol. 12, EPSC2018-1090, 2018
European Planetary Science Congress 2018

Impact ionization experiments with porous cosmic dust particle analogs

Veerle J. Sterken (1), Georg Moragas-Klostermeyer (2), Jon Hillier (3), Lee Fielding (5), Ralf Srama (2)
(1) Astronomical Institute, University of Bern, Bern, Switzerland (veerle.sterken@aiub.unibe.ch, info@veerlesterken.ch), (2) IRS, Universität Stuttgart, Germany, (3) Center for Astrophysics and Planetary Science, University of Kent, UK, (4) Faculty of Geosciences, Heidelberg University, Germany (5) School of Materials, The University of Manchester, UK

Abstract

Impact ionization dust instruments in the solar system have provided mass, velocity and directional information from impacting interplanetary and interstellar dust particles. Calibration of these instruments is usually performed with a van de Graaff dust accelerator. Most of these calibrations use relatively compact dust analogues like iron, carbon or coated minerals. In this work, we report on the preparation of low-density dust analogs, the experiments to fly these in the accelerator, and on preliminary calibration results.

Low-density dust analog preparation and experiments

Impact ionization experiments have been performed since more than 40 years for calibration of cosmic dust instruments using a linear Van de Graaff dust accelerator. Such an accelerator can accelerate conductive dust particles of sizes between about a few tens of microns, and a micron to speeds up to 80 km s^{-1} depending on particle size. Many different materials have been used for instrument calibration, from iron in the earlier days to carbon, metal-coated minerals and most recently, minerals coated with conductive polymers [1]. While different materials with different densities have been used for instrument calibration, this study focuses on a comparative analysis of compact particles versus porous or fluffy particles of the same material in specific. Porous or fluffy particles are increasingly found to be present in the solar system, e.g. dust from comet 67P Churyumov-Gerasimenko or aggregate grains from the plumes of Enceladus. Recently also indications were found for low-density interstellar dust from Stardust sample return [2], and from Ulysses interstellar dust data and trajectory simulations [3]. These recalibrations are important for determining the size distributions of interplanetary and interstellar dust.

We report on the calibrations that were performed at the Heidelberg dust accelerator facility for investigating the influence of particle density on the impact ionization charge after impact. We used the Cassini Cosmic Dust Analyser as an impact target. We explain the experiment set-up, the preparation of the materials, and the materials used: polypyrrole (PPY) coated compact, hollow silica dust particles, and carbon aerogel. Also an attempt was made to fly PPY-coated silica aerogel particles. We elaborate on the technical challenges and on the preliminary results of this work.

References

[1] Fielding, L.A., Hillier, J.K., Burchell, M.J., Armes, S.P.: Space science applications for conducting polymer particles: synthetic mimics for cosmic dust and micrometeorites. Chem. Commun., 2015, Vol. 51, pp. 16886-16899 DOI: 10.1039/c5cc07405c

[2] Westphal, A.J., et al.: Evidence for interstellar origin of seven dust particles collected by the Stardust spacecraft, Science, Vol. 345, Issue 6198, pp. 786-791, 2014.

[3] Sterken, V.J., Strub, P., Krüger, H., von Steiger, R., and Frisch, P.: Sixteen Years of Ulysses Interstellar Dust Measurements in the Solar System. III. Simulations and Data Unveil New Insights into Local Interstellar Dust, The Astrophysical Journal, Vol. 812, Issue 2, article id. 141, 24 pp., 2015.

EPSC Abstracts
Vol. 12, EPSC2018-1163, 2018
European Planetary Science Congress 2018

UPLC-MS analysis of organic matter in interstellar/cometary ice analogs

Claude Geffroy-Rodier [1] , Gregoire Danger [2], **Pauline Poinot** [1]
(1) Université de Poitiers, Institut de Chimie des Milieux et Matériaux de Poitiers (IC2MP), UMR CNRS 7285, F-86073 Poitiers, France, (2) Université Aix-Marseille, Laboratoire de Physique des Interactions Ioniques et Moléculaires (PIIM), UMR CNRS 7345, F-13397 Marseille, France

Abstract

Search for organic matter in the solar system has become a key challenge in planetary exploration in order to understand whether they played a role in the origin and evolution of life on Earth. Among the studied extraterrestrial objects, comets or analogs are uniquely pristine bodies providing characteristic insights about the formation of the Solar System. Until now, unique data were collected from GC-MS or GCxGC-MS systems and/or through direct infusion in HRMS instrument. They gave a first proxy on the ice elemental distribution and revealed that cometary ices analogs are formed of thousands of different chemical compounds. While some low molecular mass compounds (i.e. VOCs) were definitely separated and identified ($15 < m/z < 300$), higher mass peaks only gave access to the raw molecular formula of the compound. Yet, and this is particular true for high masses, one formula can be attributed to several molecules bearing highly different structures and reactivity.
Liquid chromatography coupled to a hybrid Q-Orbitrap mass spectrometer could provide a more comprehensive analysis of the cometary molecular structure by separating a large set of compounds.
In this line, this work presents the optimization stages of a novel dual-LC setup dedicated to the separation and detection in a single run of polar, apolar, monomeric, and polymeric species. The trapping and the resolving powers of its two constitutive units (preconcentration and analytical units) when separating mixtures of sugars, amino acids, nucleic acids and peptides will be presented.

1. Introduction

Many organic molecules present in interplanetary bodies such as comets and asteroids may have been delivered to the Early Earth during the heavy bombardment phase in the first hundred million years of the solar system [i] . Within this matter, some organics may have contributed to the development of self-organised molecular systems and finally to the emergence of life. Their detection in objects of the Solar System has then become a key challenge in astrobiology in order to understand their potential role in a prebiotic chemistry[ii,iii].
Up to now the technique of choice which was and is still used to investigate the molecular content of such objects is the GC-MS. For sixty years, it has been combined with diverse chemical pre-treatments to widen the range of detected compounds (i.e. from low to medium masses). Derivatisation has also provided a real value to GC-MS analysis in terms of specificity and sensitivity (detection limits about 10 µM)[iv]. Thanks to these approaches, volatile and semi-volatile building blocks of life have been detected in meteorites as well as in the Space. However, it is known that many of these sub-unites can be produced abiotically. These facts make it very difficult or even impossible to assign them a definite biological origin. Researchers are then now interested in finding molecular systems with a higher degree of organisation, resembling for instance nucleic acids or proteins (polysaccharides, polypeptides, polynucleotides, phospholipids, glycolipids, etc.). The detection of such organised systems will stand for a primitive chemical evolution of organic matter, the prelude of biochemical and replicative systems, as it took place on the Earth until the emergence of living systems.
The search for these unambiguous signatures of extant or extinct life beyond Earth has then required new inputs from the scientific community. Novel analytical strategies have then been developed to detect these so-called biomarkers in Space environments. Recently, High Resolution Mass Spectrometer analyses (HRMS) were performed to provide global analyses of interplanetary bodies or analogs. They have then delivered the elemental composition of the samples and stoichiometric formulae were attributed to ions with a m/z ratio up to 400[v]. Interestingly, few molecular masses up to 4000 $g.mol^{-1}$ were highlighted suggesting the presence of macromolecules. This striking issue was strengthened by data coming from acid hydrolysis and GC-MS analysis of the samples. Indeed, signals of the whole amino acids and diamino acids

significantly increased after HCl hydrolysis. These free monomers were thought to come from either peptide-like polymers, hydantoin or aminonitriles by-products. However, ultimate proof is still needed[vi,vii].

2. An additional section

To deepen knowledge on the molecular composition of objects of the Solar System, non-destructive analytical methods that do not rely on the volatility of organic matter are alternative valuable strategies[22]. In this line, we have developed two original LC-HRMS configurations[viii], (1) a 1D-LC-HRMS setup enabling one run analysis of a wide range of chemical families, and (2) a dual-LC-HRMS setup allowing the analysis of higher molecular weight compounds. To design the latter one, the technical functionalities of the MultiDimensional Liquid Chromatography system (two LC pumps for different retention and elution gradients) have been diverted so that our dual-LC-HRMS setup connects a series of trapping columns with analytical reverse-phase columns (Fig. 1).

When applied to laboratory cometary ice analogs, the 1D-LC-HRMS strategy has offered the opportunity to observe global fingerprints of both building block molecules and potential macromolecules without any a priori acid hydrolysis or chemical derivatisation such as performed for GCxGC-MS analysis. The dual-LC-HRMS system has efficiently differentiated higher molecular weight molecules ($350 < m/z < 600$) by increasing their signals and separating them in a resolutive manner. Indeed, as illustrated in Fig. 2, this new configuration has clearly separated and emphasised the indistinct high mass signals of high molecular weight compounds ($350 < m/z < 600$) not yet identified in cometary ice analogs[ix].

MS data processing further revealed that four ions corresponded to possible peptide sequences. This was the first identification of organised molecular systems with m/z higher than 350 in analogs of interplanetary bodies. It came to support the findings which highlighted an amplification of GC-MS signals of amino acids and dipeptides after acid hydrolysis.

3. Figures

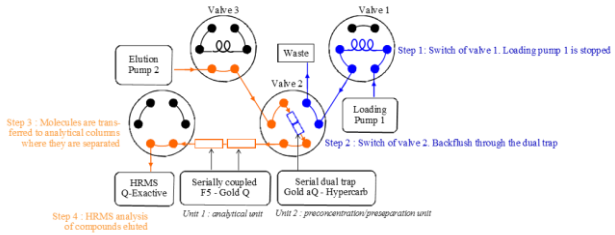

Fig. 1. Schematic representation of the dual-LC-HRMS strategy.

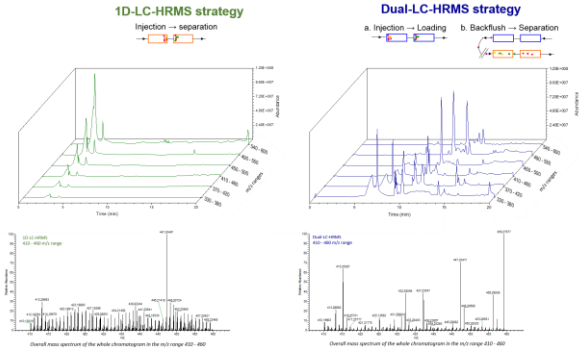

Fig. 2. TICs of a cometary analog after analysis with a 1D-LC-HRMS strategy (TICs in green) and the dual-LC-HRMS strategy (TICs in blue). The dual-LC-HRMS system worked as if the few peaks observed with the serially coupled columns were fractionated into numerous peaks. The gradual appearance and disappearance of chromatographic peaks between 9 and 11 min and 13 and 16 min in the different m/z ranges suggest an important molecular diversity in the cometary ice analog.

4. Conclusion

These data in hands, we are going to develop a targeted analysis method on a UPLC-Triple Quadrupole (TQ) instrument in order to confirm the presence of building blocks molecules and oligopeptides.

For that, the chromatographic conditions allowing an effective separation of amino acids (whatever their chirality) will be investigated (column [x], gradient elution…). Then, amino acids mass transition(s) will be determined to obtain a specific and sensitive detection. The performance hallmarks (repeatability, linearity, sensitivity…) of our novel UPLC-MS strategy will then be confronted with the ones of the derivatisation-GC-MS method currently used for the analysis of amino acids in the field of exobiology

5. Acknowledgments

This research was carried out within an exobiology technology program with the financial support of the French National Space Agency (CNES) and French

National Research Agency (CNRS council). We gratefully acknowledge Frédéric Courtade for her implication in this program. We also thank Guillaume Boulissière for its help during one of the experimental plans. This work was also funded by the French national programs « Physique Chimie du Milieu Interstellaire » (P.C.M.I, Institut National des Sciences de l'Univers, Centre National de la Recherche Scientifique) and « Programme National de Planétologie » (P.N.P, INSU-CNRS). This work was further supported by the ANR project RAHIIA_SSOM (Grant ANR-16-CE29-0015-01), the ANR project VAHIIA (Grant ANR-12-JS08-0001), the ANR project PeptiSystems (Grant ANR-14-CE33-0020-02) and finally by the Foundation of Aix-Marseille University.

6. References

[i] C. Chyba, et al. Science. 249 (1990) 366. doi:10.1126/science.11538074.
[ii] B.R. Simoneit et al. Orig. Life Evol. Biosph. 28 (1998) 475–483.
[iii] W.M. Irvine. Orig. Life Evol. Biosph. 28 (1998) 365–383.
[iv] R. Navarro-González et al. Proc. Natl. Acad. Sci. 103 (2006) 16089–16094. doi:10.1073/pnas.0604210103.
[v] T. Gautier et al. Icarus. 275 (2016) 259–266. doi:10.1016/j.icarus.2016.03.007.
[vi] M. Nuevo et al. Orig. Life Evol. Biospheres. 38 (2008) 37–56.
[vii] K. Kobayashi et al. Adv. Space Res. 16 (1995) 21–26. doi:10.1016/0273-1177(95)00188-K.
[viii] B. Eddhif et al. Talanta. 179 (2018) 238-245. doi: 10.1016/j.talanta.2017.11.008.
[ix] R.I. Kaiser et al. Astrophys. J. 765 (2013) 111. doi:10.1088/0004-637X/765/2/111.
[x] W. Van Helmond et al. Anal. Methods. 9 (2017) 5697–5702. doi: 10.1039/c7ay01603d.